Astron. Astrophys. 356, 849–872 (2000)

ASTRONOMY AND ASTROPHYSICS

Multi-colour PL-relations of Cepheids in the HIPPARCOS catalogue and the distance to the LMC⋆

M.A.T. Groenewegen[1] **and R.D. Oudmaijer**[2,3]

[1] Max-Planck Institut für Astrophysik, Karl-Schwarzschild-Strasse 1, 85740 Garching, Germany
[2] Department of Physics and Astronomy, University of Leeds, LS2 9JT Leeds, UK
[3] Blackett Laboratory, Imperial College of Science, Technology and Medicine, Prince Consort Road, London SW7 2BZ, UK

Received 10 November 1999 / Accepted 3 February 2000

Abstract. We analyse a sample of 236 Cepheids from the HIPPARCOS catalog, using the method of "reduced parallaxes" in V, I, K and the reddening-free "Wesenheit-index". We compare our sample to those considered by Feast & Catchpole (1997) and Lanoix et al. (1999), and argue that our sample is the most carefully selected one with respect to completeness, the flagging of overtone pulsators, and the removal of Cepheids that may influence the analyses for various reasons (double-mode Cepheids, unreliable HIPPARCOS solutions, possible contaminated photometry due to binary companions).

From numerical simulations, and confirmed by the observed parallax distribution, we derive a (vertical) scale height of Cepheids of 70 pc, as expected for a population of 3-10 $M_\odot$ stars. This has consequences for Malmquist- and Lutz-Kelker (Lutz & Kelker 1973, Oudmaijer et al. 1998) type corrections which are smaller for a disk population than for a spherical population.

The V and I data suggest that the slope of the Galactic PL-relations may be shallower than that observed for LMC Cepheids, either for the whole period range, or that there is a break at short periods (near $\log P_0 \approx 0.7 - 0.8$).

We stress the importance of two systematic effects which influence the distance to the LMC: the slopes of the Galactic PL-relations and metallicity corrections. In order to assess the influence of these various effects, we present 27 distance moduli (DM) to the LMC. These are based on three different colours (V, I, K), three different slopes (the slope observed for Cepheids in the LMC, a shallower slope predicted from one set of theoretical models, and a steeper slope as derived for Galactic Cepheids from the surface-brightness technique), and three different metallicity corrections (no correction as predicted by one set of theoretical models, one implying larger DM as predicted by another set of theoretical models, and one implying shorter DM based on empirical evidence). We derive DM between 18.45 ± 0.18 and 18.86 ± 0.12. The DM based on K are shorter than those based on V and I and range from 18.45 ± 0.18 to 18.62 ± 0.19, but the DM in K could be systematically too low by about 0.1 magnitude because of a bias due to the fact that NIR photometry is available only for a limited number of stars.

From the Wesenheit-index we derive a DM of 18.60 ± 0.11, assuming the observed slope of LMC Cepheids and no metallicity correction, for want of more information.

The DM to the LMC based on the parallax data can be summarised as follows. Based on the PL-relation in V and I, and the Wesenheit-index, the DM is
$18.60 \pm 0.11 \ \ (\pm 0.08 \ \mathrm{slope})(^{+0.08}_{-0.15} \ \mathrm{metallicity}),$
which is our current best estimate. Based on the PL-relation in K the DM is $\quad 18.52 \pm 0.18$
$(\pm 0.03 \ \mathrm{slope})(\pm 0.06 \ \mathrm{metallicity})(^{+0.10}_{-0} \ \mathrm{sampling \ bias}).$
The random error is mostly due to the given accuracy of the HIPPARCOS parallaxes and the number of Cepheids in the respective samples. The terms between parentheses indicate the possible systematic uncertainties due to the slope of the Galactic PL-relations, the metallicity corrections, and in the K-band, due to the limited number of stars. Recent work by Sandage et al. (1999) indicates that the effect of metallicity towards shorter distances may be smaller in V and I than indicated here.

From this, we point out the importance of obtaining NIR photometry for more (closeby) Cepheids, as for the moment NIR photometry is only available for 27% of the total sample. This would eliminate the possible bias due to the limited number of stars, and would reduce the random error estimate from 0.18 to about 0.10 mag. Furthermore, the sensitivity of the DM to reddening, metallicity correction and slope are smallest in the K-band.

Key words: stars: distances – stars: variables: Cepheids – galaxies: Magellanic Clouds – cosmology: distance scale

1. Introduction

Cepheids are important standard candles in determining the extra-galactic distance scale. The results of the HIPPARCOS mission allow, in principle, a calibration of the period-luminosity relation based on the available parallaxes. Feast & Catchpole (1997; hereafter FC) did just that for the $M_\mathrm{V} - \log P$-relation

Send offprint requests to: Martin Groenewegen (groen@mpa-garching.mpg.de)

⋆ Based on data from the ESA HIPPARCOS astrometry satellite.

based on pre-released HIPPARCOS data of 223 Cepheids available to them at that time. Now that the entire catalog has become available (ESA 1997) it is timely to analyse the full sample of Cepheids in it.

In a recent paper, Lanoix et al. (1999, hereafter L99) presented a study similar to ours and they derived the zero points of the $M_{\rm V} - \log P$- and $M_{\rm I} - \log P$-relations, without, however, discussing the distance to the LMC. We will indicate where the two studies agree and differ.

The paper is organised as follows. In Sect. 2 the sample considered in the present paper is presented, and compared to that in FC and L99. In Sect. 3 several aspects involved in the analysis of parallax data are described, and the method of "reduced parallaxes" is outlined, together with all necessary recipes to obtain the reddening. In Sect. 4 the zero points of the PL-relations in V, I, K and the reddening-free "Wesenheit-index" (e.g. Tanvir 1999, and Eq. (11)) are presented for different selections of the sample, which are discussed in Sect. 5. In Sect. 6 we construct and present the zero points for volume complete samples of stars. In Sect. 7 we describe numerical simulations that are first of all tuned to fit the observed properties of the Cepheids in the HIPPARCOS catalog, and then are used to show that the method of "reduced parallaxes" introduces a bias which is of the order of 0.01 mag or less. Based on these results we discuss in Sect. 8 the distance to the LMC, and elaborate on the various uncertainties.

2. Sample selection

The number and some properties of the Cepheid population in the HIPPARCOS catalog were discussed by Groenewegen (1999, hereafter G99). To summarise: by cross-correlating the general HIPPARCOS database, the HIPPARCOS "resolved variable catalog" and the electronic database of Fernie et al. (1995; hereafter F95), a total of 280 Cepheids was identified. Then, 9 Type II Cepheids, 1 factual RR Lyrae variable, 1 CH-like carbon-rich Cepheid, 10 double-mode Cepheids, 7 Cepheids with an unreliable HIPPARCOS solution and 4 Cepheids with no or unreliable optical photometry were excluded. Note that for RY Sco and Y Lac we use the new determinations for the parallax and its error from Falin & Mignard (1999). This leaves 248 stars, of which 32 are classified as overtone pulsators by F95, Antonello et al. (1990) or Sachkov (1997). Luri et al. (1999) have classified Cepheids in fundamental and overtone pulsators using the HIPPARCOS lightcurves, but did not yet publish the results for individual stars. For the sample, G99 calculated intensity-mean I (on the Cousins system) and $V - I$ magnitudes for 189 stars, and collected magnitude-mean colours for additional 14 stars, and provided JHK intensity-mean magnitudes on the Carter system for 69 stars.

By comparison, the FC dataset consisted of 223 stars of which 3 were discarded. These were DP Vel for lack of photometric data, and AW Per and AX Cir because they are in binaries and the photometry might be affected by the companions. However, in the F95 catalog there are many more stars which are flagged for this reason. From the sample in G99 are therefore excluded the stars flagged "O C" (RX Cam, AW Per, T Mon, SS CMa, S Mus, AX Cir, W Sgr, V350 Sgr, U Aql, SU Cyg, V1334 Cyg) and "O: C" (VY Car) in F95. This leaves 32 overtone pulsators and 204 fundamental mode pulsators in the sample considered here. They are listed for completeness in Appendix A together with some adopted parameters.

Recently, L99 also studied the Cepheids in the HIPPARCOS catalog. They selected stars listed as "DCEP" or "DCEPS" from the HIPPARCOS catalog. Interestingly, they state that they selected 247 stars, while in reality there are 250 such stars (G99). After removing 9 Cepheids for which there is no photometry listed in F95, their final sample consists of of 238 stars (including 31 overtones). They did not eliminate double-mode Cepheids, Cepheids where the photometry is (likely) contaminated by a binary companion or Cepheids with unreliable HIPPARCOS solutions. Furthermore, they assumed all Cepheids classified as "DCEPS" to be overtone pulsators, which is not the case. Their sample therefore includes stars they consider overtones which we and FC consider fundamental mode pulsators (e.g., SZ Cas, Y Oph, V496 Aql, V924 Cyg, V532 Cyg), and stars they consider fundamental mode pulsators which are overtone pulsators (e.g., V465 Mon, DK Vel, V950 Sco, see Mantegazza & Poretti 1992). In addition, V473 Lyr is considered by them to be a first overtone pulsator, while it probably is a second overtone pulsator (Van Hoolst & Waelkens 1995; Andrievsky et al. 1998; also see below).

Of the 236 stars in our sample there are 198 in common with the sample of FC. In other words, 22 stars in the FC sample would not have made it through the selection process outlined in G99 and here. Specifically, their sample contains 7 stars with unreliable HIPPARCOS solutions (we use the improved parallax values for RY Sco and Y Lac from Falin & Mignard (1999), information which was not available to FC), 9 binaries (in addition to AW Per and AX Cir) where the photometry may be contaminated by the companions and 8 double-mode Cepheids. Another difference is that 7 more stars than in FC are flagged as overtone pulsators following F95 and Sachkov (1997).

For the 198 stars in common we have compared the intensity-mean V and $B - V$. FC mention that they use F95, except when the data were in Laney & Stobie (1993). Our photometry was at first instance taken solely from F95, except for RW Cas (see discussion in G99). In V, the photometry is identical for 165 stars. For 18 stars V differs by > 0.01mag, for 8 by > 0.02mag and for 5 by > 0.03mag. The latter cases were inspected individually.

For RW Cas the difference in the sense "Fernie et al $-$ FC" is 0.101 mag. As discussed in G99, there may be a typographical error in F95.

For X Pup the difference is -0.047. The F95 entry of V = 8.460 is close to the value derived in G99 for the dataset of Moffett & Barnes (1984). The other dataset considered in G99 gives a value of $V = 8.536$. The value by FC of $V = 8.507$ is intermediate. We have kept the F95 value.

For AQ Pup the difference is 0.122 mag. G99 calculated V, I for 3 data sets. The entry in F95 ($V = 8.791$) is identical to the Moffett & Barnes (1984) dataset. The FC value of $V = 8.669$ is

close to the 2 other datasets (8.676, 8.686 mag), and one of these was the preferred one in G99 regarding the V, I photometry. For AQ Pup we use the V and $B-V$ from FC.

For RS Pup the difference is -0.081. The value in F95 (V = 6.947) is clearly off from both values in G99 (6.999 and 7.020 mag) which both are in agreement with the value of V = 7.028 used by FC. For RS Pup we use V and $B-V$ from FC.

For S Nor the difference is -0.032. The value used by FC is extremely close to the value derived in G99, and for S Nor we use the V and $B-V$ from FC.

After these changes in V and $B-V$, there are 164 with identical values for $B-V$, for 12 stars $B-V$ differs by > 0.014 mag, for 9 by > 0.028 mag, and for 5 by > 0.042 mag (RW Cas, X Pup, U Nor, RY Sco, RU Sct). These cases have not been considered separately. It merely indicates that errors in V and $B-V$ (and hence reddening) can contribute to the uncertainties in the derivation of the zero point of the PL-relation, as will be discussed below.

For V1162 Aql, we discovered an error in the $(B-V)$ value listed in F95. From the data in Berdnikov & Turner (1995) that was used in G99 to calculate $(V-I)$ we derive and adopt an intensity weighted mean of $(B-V)$ = 0.879 magnitudes.

In G99, V and I photometry was presented for many Cepheids in the HIPPARCOS catalog, based on a literature search. When possible, intensity-mean magnitudes were calculated based on the original published datasets. Some magnitude-means were also presented. The $V-I$ magnitudes are taken from G99. When there are multiple entries the first one was taken following the considerations in G99. In total there is I-band data for 191 stars (or 81% of the sample), 178 of which are intensity-mean magnitudes. In G99 it was shown that there is no significant difference between the intensity-mean and magnitude-mean, and so the remaining 13 magnitude-means are used without correction.

G99 also presented intensity-mean JHK magnitudes in, or transformed to, the Carter system. When there are multiple entries the first one is taken, following the considerations in G99. In total there is JHK-band data for 63 stars, or 27% of the sample.

3. Analysing parallax data

Analysing parallax data is not a trivial exercise, and has led to some confusion in the literature. Part of this confusion is probably related to the fact that parallax data suffer from many types of biases (see Brown et al. 1997). For example, the most conspicuous bias, the Lutz-Kelker (LK; Lutz & Kelker 1973) bias, although known for a long time, could not be empirically investigated due to a lack of data on which it could be tested.

One can visualize the LK effect by analogy with the well-known Malmquist bias. Malmquist bias occurs on samples of objects because due to a particular magnitude cut, objects that are brighter than the mean will be included in a sample, while objects that are fainter than the mean will be excluded. The net effect of this type of bias is that the intrinsic magnitude for a certain sample will be too bright if no corrections are applied. To investigate the presence of such biases, one can look at so-called Spaenhauer diagrams, where the observed magnitude is plotted as a function of, for example, distance. In such a way it is relatively easy to find the point where the Malmquist bias starts to dominate (see e.g. Sandage 1994).

A similar, but opposite effect, is due to the LK bias. For a given parallax cut (or any selection based on the parallax, or its associated error), on average, more objects that are located far away will scatter into the sample, than stars will scatter out of the sample, as the sampled volume is larger for the former objects. Because the distances to the objects scattered into the sample are then underestimated, this effectively results in a too faint mean 'intrinsic' magnitude of the entire sample. As with the Malmquist bias, the LK-bias depends on the space distribution of the sample of stars under consideration. Contrary also to the Malmquist bias is that although the error-bars on the parallax are symmetric, those on the derived distances and intrinsic magnitudes are a-symmetric, which seriously affects the analysis of the data. In addition, the relative error-bars on the parallax increase with distance.

The LK bias was shown to exist empirically by Oudmaijer et al. (1998). Fig. 1 gives an illustrative plot, showing the magnitudes of the Cepheids under consideration, derived from their photometry and observed parallax, as a function of parallax in the upper panel, and as function of relative error in the lower panel ($\rho = V_0 + 5\log\pi + 5 - \delta\log P$, for $\delta = -2.81$ – see next section for details). As the absolute error in the HIPPARCOS data is more or less constant, the two figures are equivalent. The inferred magnitude of the objects in the Cepheid sample is not a random distribution around the mean, but shows a clear trend as function of parallax. For large parallaxes (and small relative errors) the inferred magnitudes are too faint, and then, for larger distances, the objects become too bright. It was only in Oudmaijer et al. (1998), that this was shown empirically for the first time.

Indeed, it is clear from this type of graph, which is a version of a Spaenhauer diagram, that a selection on parallax (or relative error in parallax) will not return the correct answer. In most cases the result will be biased (but see Oudmaijer et al. 1999, for a counter-example).

Lutz & Kelker (1973) were the first to investigate this effect, and found that the resulting bias can be substantial, increasing with increasing relative error. For a relative error of 17.5% in the parallax, the bias is 0.43 magnitudes – yet as Koen (1992) later showed, the confidence intervals around these corrections are large. The 17.5% limit was taken literally by subsequent authors, and often stars with worse determinations were deleted or individual stars were corrected with the values LK derived.

LK claimed that individual stars suffer from the same bias, a point they emphasize strongly. Actually, it is quite a surprising result that LK concluded that individual stars are biased. LK start their calculations assuming that the observed parallax equals the true parallax with a random error, a standard procedure when investigating measurement errors and the main assumption for Monte-Carlo simulations as performed in e.g. Sect. 7 of this paper. It seems rather contradictory then that LK infer from their

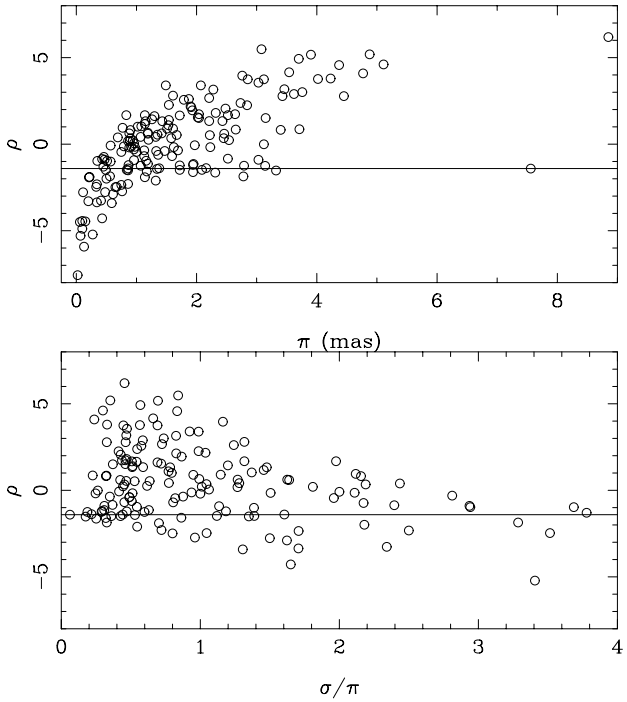

Fig. 1. $\rho = V_0 + 5\log\pi + 5 - \delta\log P$ plotted against parallax, and relative parallax error, for the stars with positive observed HIPPARCOS parallaxes. For comparison the derived value for the zero point ρ derived for the full sample (Table 1, solution 10) is indicated.

results that individual stars are biased if their initial conditions assume otherwise.

Let us first comment on whether the conjecture that the observed parallax is equal to the true parallax (plus a random observational error) is correct. It is actually quite hard to investigate this in a 'bias-free' manner, but the evidence provided by the HIPPARCOS mission swings the balance towards answering this question with a 'yes'. Measurements of stars beyond the detection limit of HIPPARCOS, such as those in the Magellanic Clouds (Van Leeuwen 1997, Arenou et al. 1995) consistently give average observed parallaxes close to zero mas with a scatter of order the observational error. This indicates that the measurements are not biased, even though the relative errors on the parallax are substantial – and the results for individual stars can be widely off the true distance, but crucially, in the mean they appear to give the right answer within the errors rather than show a conspicuous bias in one direction. In addition, analyses of Open Clusters, for which photometric distances are known, do not show a deviation from the mean distance for increasing distances and thus lower quality data (Arenou et al. 1995, Robichon et al. 1999). Based on this, it appears that individual stellar determinations are most likely not biased.

There is one exception, mentioned briefly by Koen & Laney (1998). These authors argue that if a single star is the result of a selection on parallax, its measurement is biased. Although this sounds counter-intuitive, it is a formal implication from the fact that a selection on parallax gives rise to a bias.

A final comment concerns the use of parallaxes of a sample of which one does not know that the objects should have the same intrinsic magnitude, while their distances are not known. The trend observed in Fig. 1 that, for a given sample, large parallaxes return in principle too faint intrinsic magnitudes, while small parallaxes return too bright magnitudes, can have serious implications in the interpretation of the data.

3.1. How to deal with the Lutz-Kelker bias?

The remaining question is how one should deal with the effects of the bias. Should one, as often the case with Malmquist bias, introduce a (sample-dependent) correction factor, or are there ways to circumvent the problem?

In a paper dealing with this problem, Turon Lacarrieu & Crézé (1977) discuss two different methods: [1]

Accepting that a sample selected on parallax is inevitably biased, they first considered using the better parallaxes, and investigate the resulting mean magnitudes, and provide corrections along similar lines as LK (also see Smith 1987a,b,c, Koen 1992).

Secondly they considered a full sample, and, avoiding transformations from parallaxes to distances and magnitudes, they derive the mean parallax first and use the resulting mean parallax to derive the mean magnitude of the sample. Since negative parallaxes can not be incorporated into a mean magnitude, one in principle has to discard these data, in effect selecting on parallax and thus biasing the sample. Therefore, Turon Lacarrieu & Crézé (1977) introduced the so-called "reduced parallax" ($10^{0.2M_V} \sim \pi$), which can take into account negative parallaxes, and hence the (weighted) mean of the reduced parallax can be converted into a mean magnitude. This method, as will be discussed in Sect. 3.2, indeed appears to be "bias-free", mainly because a weighting scheme puts less weight on the larger deviations around the mean from the lower quality data, whilst not being a formal selection on parallax.

The Cepheids in HIPPARCOS were investigated previously by FC who used the second, reduced parallax method, and Oudmaijer et al. (1998), who used a scheme based on the first method. Their results were equal within the error-bars. Although FC used the reduced parallax method, which formally does not suffer from LK bias (Koen & Laney 1998), they still suggested in a footnote that a LK correction of 0.02 mag should be applied on their final result. This is not necessary; the result only has to be corrected for Malmquist bias, as FC also pointed out, but did not actually apply, as they estimated it would essentially counteract their proposed LK correction of 0.02 mag.

These, and other issues will be investigated in the remainder of this paper. First, we will outline the method for the reduced parallaxes again.

[1] Note that Turon Lacarrieu & Crézé (1977) repeat the phrase by LK that 'individual stars' suffer from the bias, without specifying whether this would mean *all* stars (which contradicts their own assumption that the observed parallax is equal to the true parallax with an associated error-bar), or individual stars that are the result of a selection on parallax.

3.2. The "reduced parallax" method

The method of "reduced parallax" (discussed by Turon Lacarrieu & Crézé 1977) was the one used by FC in analysing Cepheid data.

Consider a Period-Luminosity relation of the form:

$$M_{\rm V} = \delta\ \log P + \rho, \tag{1}$$

where P is the fundamental period in days. If $\langle V\rangle$ is the intensity-mean visual magnitude and $\langle V_0\rangle$ its reddening corrected value, then one can write:

$$10^{0.2\rho} = \pi \times 0.01\ \ 10^{0.2(\langle V_0\rangle - \delta\ \log\ P)} \equiv \pi \times {\rm RHS}, \tag{2}$$

which defines the expression RHS and where π is the parallax in milli-arcseconds. This method has the advantage that negative parallaxes can be used in the analyses as well. A weighted-mean, with error, of the quantity $10^{0.2\rho}$ is calculated, with the weight (weight = $\frac{1}{\sigma^2}$) for the individual stars derived from:

$$\sigma^2 = (\sigma_\pi \times {\rm RHS})^2 + (0.2\ \ln(10)\ \ \pi\ \sigma_{\rm H} \times {\rm RHS})^2\,, \tag{3}$$

with σ_π the standard error in the parallax. This follows from the propagation-of-errors in Eq. (2). For the error (denoted $\sigma_{\rm H}$) in $(\langle V_0\rangle - \delta\ \log\ P)$ we follow FC's "solution B" and adopt $\sigma_{\rm H} = 0.1$ throughout this paper. Recently, L99 considered alternative weighting schemes, but concluded that the one used by FC and the present paper gives the most reliable zero point and the lowest dispersion.

The reddening is derived as follows. The intrinsic colours follow from the relation in Laney & Stobie (1994):

$$\langle B\rangle_0 - \langle V\rangle_0\ = 0.416\ \log P + 0.314, \tag{4}$$

which has a dispersion of 0.091 mag. The visual extinction ($A_{\rm V} = R_{\rm V} \times E(B-V)$) is calculated using (Laney & Stobie 1993):

$$R_{\rm V} = 3.07 + 0.28\ (B-V)_0 + 0.04\ E(B-V). \tag{5}$$

No dispersion is given for this relation, only an error of 0.03 in the zero point. We will assume that the dispersion in Eq. (5) is slightly larger than this, namely 0.05 mag.

For overtone pulsators, the fundamental period has to be estimated from the observed period. This was done, following FC, using:

$$P_1/P_0 = 0.716 - 0.027\ \log P_1, \tag{6}$$

with a dispersion we estimate from the original data (Alcock et al. 1995) to be of order 0.002.

For pulsators in the second overtone, the fundamental period is calculated, following FC, using:

$$P_2/P_0 = 0.55. \tag{7}$$

This completes the description of the method used by FC.

Alternative methods which are described now, follow this description closely but are based on $\langle V\rangle$ and $\langle I\rangle$, respectively $\langle J\rangle$ and $\langle K\rangle$ photometry instead of $\langle B\rangle$ and $\langle V\rangle$. The rationale being that the extinction in I and K is less than in V, and that the scatter in the $M_{\rm I} - P$- and $M_{\rm K} - P$-relations is less than in the $M_{\rm V} - P$-relation (Tanvir 1999, Laney & Stobie 1994).

First consider the case based on V and I. The intrinsic colour is derived from (Caldwell & Coulson 1986):

$$\langle V\rangle_0 - \langle I\rangle_0\ = 0.292\ \log P + 0.443 \tag{8}$$

which has a dispersion of 0.064 mag. This relation was derived for magnitude-mean $(V-I)_0$ but we will assume it to hold for intensity-mean magnitudes as well. In a recent paper, Feast (1999, Appendix D), presents a correction formula that implies that the difference intensity-mean minus magnitude-mean $(V-I)$ colour is of order -0.017 mag for a typical V-band amplitude of 0.7 mag.

There seems not to exist a relation similar to Eq. (5), where $R(I) \equiv A_{\rm I}/E(V-I)$ is related to $(\langle V\rangle - \langle I\rangle)_0$ and/or $E(V-I)$. We have derived such a relation from the available BVI data.

For each star with BVI photometry, $(\langle B\rangle - \langle V\rangle)_0$ and $(\langle V\rangle - \langle I\rangle)_0$ can be calculated from Eqs. (4) and (8). Then, $A_{\rm I}$ is calculated using Gieren et al. (1998):

$$R_{\rm I} = 1.82 + 0.205\ (B-V)_0 + 0.022\ E(B-V), \tag{9}$$

and $A_{\rm I} = R_{\rm I} \times E(B-V)$. In Fig. 2 $R(I)$ is plotted versus $(V-I)_0$. A least-square fit to 183 data points gives:

$$R(I) = 1.422 \tag{10}$$

with no significant dependence on $(V-I)_0$ and with a standard error of 0.19. For $\sigma_{\rm H}$ (in this case the error in $(\langle I_0\rangle - \delta_{\rm I}\ \log\ P)$) we adopt a value of 0.15 mag (Tanvir 1999).

A variation on this method that treats the problem of reddening in a different way, is to use the reddening-free so-called "Wesenheit-index" (see for example Tanvir 1999), that uses the *observed* colours but is essentially reddening-free when defined as:

$$W = V - 2.42\ (V-I). \tag{11}$$

For $\sigma_{\rm H}$ (in this case the error in $(\langle W\rangle - \delta_{\rm W}\ \log\ P)$) we adopt a value of 0.11 mag (Tanvir 1999).

Now consider the case based on J and K colours. The intrinsic color is derived from Laney & Stobie (1994):

$$\langle J\rangle_0 - \langle K\rangle_0\ = 0.149\ \log P + 0.310 \tag{12}$$

which has a dispersion of 0.044 mag. Again, there seems not to exist a relation similar to Eq. (5), where $R(K) \equiv A_{\rm K}/E(J-K)$ is related to $(\langle J\rangle - \langle K\rangle)_0$ and/or $E(J-K)$. We have derived such a relation from the available $BVJK$ data.

For each star with $BVJK$ photometry, $(\langle B\rangle - \langle V\rangle)_0$ and $(\langle J\rangle - \langle K\rangle)_0$ can be calculated from Eqs. (4) and (12). Then, $A_{\rm K}$ is calculated using Laney & Stobie (1993):

$$A_{\rm K} = 0.279\ E(B-V). \tag{13}$$

In Fig. 3 $R(K)$ is plotted versus $(J-K)_0$. A least-square fit to 55 data points gives:

$$R(K) = 1.035 - 1.063\ (J-K)_0 \tag{14}$$

with a standard error of 0.091. For $\sigma_{\rm H}$ (in this case the error in $(\langle K_0\rangle - \delta_{\rm K}\ \log\ P)$) we adopt a value of 0.12 mag (Gieren et al. 1998).

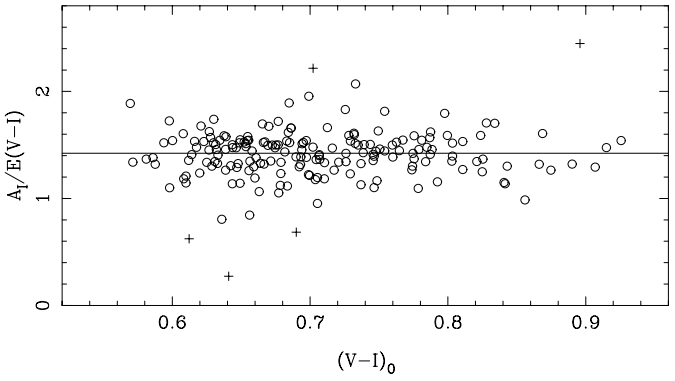

Fig. 2. The relation between $R(I)$ and $(\langle V\rangle - \langle I\rangle)_0$. The fit reported in Eq. (10), is based on 183 stars. Eight outliers (the crosses) were not considered in the fit. Three outliers are outside the plot range. There is no dependence on $(V-I)$.

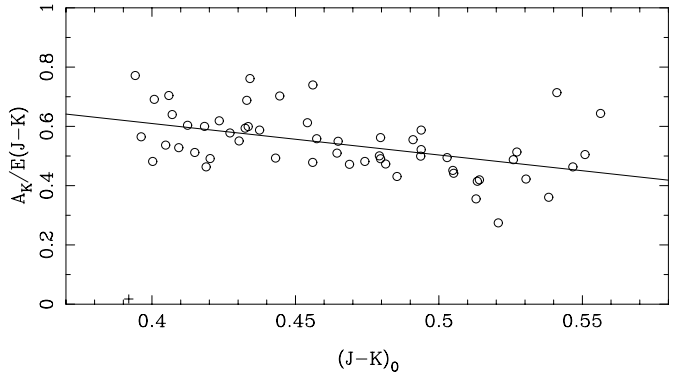

Fig. 3. The relation between $R(K)$ and $(\langle J\rangle - \langle K\rangle)_0$. The fit reported in Eq. (14), is based on 55 stars. Eight outliers (the crosses) were not considered in the fit. Seven outliers are outside the plot range. There is a dependence on $(J-K)$.

4. Zero points of the PL-relations

4.1. Zero point of the $M_{\rm V} - \log P$-relation

In Tables 1-4 we present the results from the "reduced parallax" method presented in the previous section for different samples of stars, and based on different colors (BV, VI or JK). To test the implementation of the method we have calculated the zero point for some of the solutions considered in FC, adopting a slope $\delta = -2.81$ and working with BV colours, as they did. The data for the sample used by FC come from Feast & Whitelock (1997; their Table 1). These are our solutions 1-7 in Table 1, and the value for the zero point and total weight are in perfect agreement to within the listed number of decimal places in FC. The error in the zero point determination is slightly different, ours being larger by a few 1/100-th of a magnitude. Using the FC sample, we also calculated the solution for the overtones only, and the overtones excluding Polaris (solutions 8-9).

For the present sample and using a slope $\delta = -2.81$ solutions 10-12 give the value for the zero point for the whole sample, and for fundamental mode and overtone pulsators separately. In this case, V473 Lyr was considered to be pulsating in the second overtone. This interesting object is thought to be the only Galactic Cepheid pulsating in the second overtone (Van Hoolst & Waelkens 1995 and Andrievsky et al. 1998). The values of ρ assuming that V473 Lyr is a fundamental mode, first overtone or second overtone pulsator, respectively, are -2.68, -2.07 and -1.61, all with an error of 0.70. With such a large error only fundamental mode pulsation can be excluded from the HIPPARCOS parallax alone. The zero point assuming second overtone pulsation is consistent with the zero point obtained for the whole sample, and we will hence assume in our zero point determinations that V473 Lyr is indeed a second overtone pulsator.

The zero point for the entire sample of -1.41 ± 0.10 compares to the value of FC of -1.43 ± 0.10, and the value of L99 of -1.44 ± 0.05 (they used a slightly different slope of -2.77). These values are all very similar, and the differences are mainly due to the different samples of Cepheids, and to a lesser extent to the slight differences in the adopted photometry. We believe that the present sample is the most carefully selected sample of the three with respect to completeness, the flagging of overtone pulsators, and the removal of Cepheids that may influence the analysis for various reasons (double-mode Cepheids, unreliable HIPPARCOS solutions, possible contaminated photometry due to binary companions), as explained in the introduction.

4.1.1. P_0 versus P_1

A first comment is on the different solution from the fundamental mode and overtone pulsators. In FC the difference between the solution using the fundamental pulsators or the full sample was only 0.02 mag. In our case it is about 0.08. FC did not present the solution for the overtones only, but we have calculated it from their data (solution 8). The difference using only the overtones or the fundamental pulsators is 0.05 mag in their case. In our case it is 0.15 mag, which is a difference at the 1σ level. This indicates how important it is to carefully flag the overtone pulsators.

4.1.2. Selecting on visual magnitude

L99 derive a zero point of -1.44 (after correcting for a bias of -0.01 mag) with a very small error of 0.05, using a selection on $V \leq 5.5$. We confirm (solutions 14 and 15) that the derived zero point is not significantly different from that for the whole sample, but we do not confirm such a small error. In fact, Pont (1999) argues that the error of 0.10 in FC is even underestimated based on his numerical simulations. Our simulations confirm this (Sect. 7) and so it is not clear how L99 arrived at such a small error.

4.1.3. Selecting on parallax

For solutions 16-18 only positive parallaxes have been selected to highlight the effect of LK-bias. The zero points are fainter, as expected. Interestingly enough, the zero point for the overtone pulsators is hardly changed. Only 5 overtones (15%) have

negative observed parallaxes and those carry very little weight, while for the fundamental mode pulsators a selection on positive parallaxes reduces the number by 32%.

4.1.4. Selecting on weight

FCs final choice for the zero point relied heavily on a subsample of 26 stars, selected on weight. The question arises if this introduces some bias. For solutions 19-24 we have made different selections on weight, in particular solutions 19-22 have been devised such that each bin selected on individual weight has about the same total weight, so that the errors on the zero point are comparable. The differences are at the 1σ level. From numerical simulations performed in Sect. 7 (see Table 6) we confirm that there are no indications at the present level of accuracy that a selection on weight is an (indirect) selection on parallax, and so a sample selected on weight appears not to be subject to LK-bias. The error on the zero point determination is larger when selecting on (individual) weight, simply because of the smaller value of the total weight (see Table 6). This is different from the result in FC, who quote a *smaller* error on the zero point for the sample selected on weight compared to their full sample (cf. their solution 6 and 1).

4.1.5. Selecting on period

Solutions 25-36 represent cases where the sample was split up in bins in $\log P$ carrying approximately equal weight, for the whole sample (solutions 25-28), and the fundamental pulsators only (solutions 29-32, and 33-36 for a slope of -2.22). In both cases, the star with the highest individual weight was excluded in defining the bins. There is a significant dependence of the zero point on $\log P$. This is particularly clear in the case of the fundamental mode pulsators where the zero point for stars with $\log P \geq 0.85$ differs at the 3σ level from the shortest period bin.

To expand on this matter further, we show in Fig. 4 how $10^{0.2\rho}$ depends on $\log P$ for the full sample (top panel), and for the 47 stars with an individual weight > 5. Shown are the weighted-mean values of $10^{0.2\rho}$ (solid lines), and weighted least-square fits to the data of the form $10^{0.2\rho} = \alpha \log P + \beta$ (dashed line). The (α, β) found are (0.11 $\pm$ 0.12, 0.44 $\pm$ 0.10) for the full sample, and (0.094 $\pm$ 0.115, 0.43 $\pm$ 0.09) for the 47 stars. The analysis was repeated for the fundamental mode pulsators only, giving samples of 204 and 35 stars, respectively. The (α, β) found are (0.17 ± 0.15, 0.35 ± 0.14) for the full sample, and (0.17 $\pm$ 0.15, 0.34 $\pm$ 0.14) for the stars with weight > 5. The slopes derived are significant at the 1σ level only.

These results depend on the adopted slope in the PL-relation. For a slope $\delta = -3.1$ we find that the effect of the dependence of the zero point on the binning in $\log P$ is enhanced, and that the slope in the $10^{0.2\rho}$ versus $\log P$ relation becomes significant at the 2σ level. We also calculated the results for a slope of $\delta = -2.22$ (Bono et al. 1999). The results are listed as solutions 33-36 for the fundamental pulsators. The dependence on period is not significant in this case, although

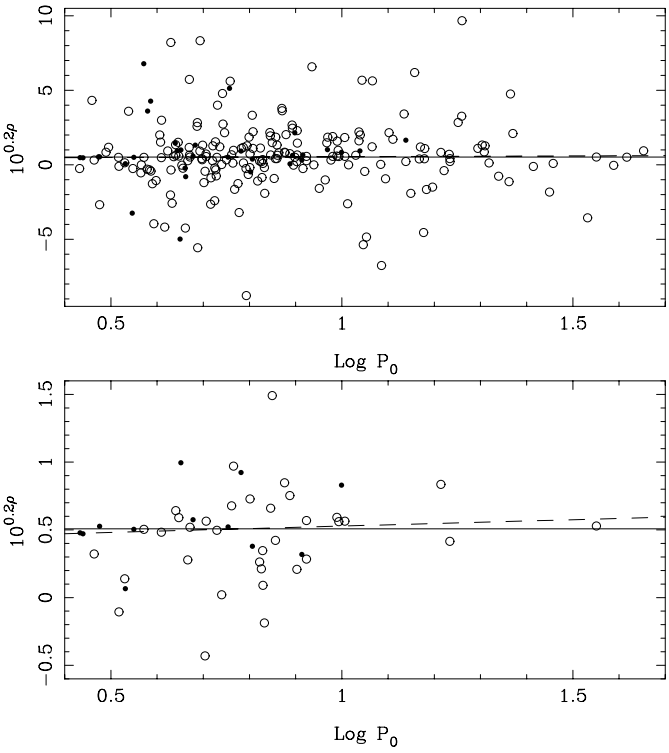

Fig. 4. $10^{0.2\rho}$ versus $\log P$ based on BV colours for a slope of -2.81. In the top panel all 236 stars are plotted. The overtones are marked by the filled symbols. In the bottom panel only the 47 stars with an individual weight > 5 are shown. The solid lines represent the weighted mean of $10^{0.2\rho}$ for the respective samples. The dashed lines represent the weighted least-squares fit to the data for the respective samples (see text). This provides weak evidence that the slope of -2.81 is too steep.

the shortest bin remains the brightest. Least-square fits give the following results for (α, β): all stars (-0.039 ± 0.090, 0.45 ± 0.08), 56 stars with weight > 5 (-0.050 ± 0.099, 0.45 ± 0.08), all fundamental pulsators (0.00 ± 0.11, 0.39 ± 0.11), 42 fundamental pulsators with weight > 5 (0.00 ± 0.13, 0.38 ± 0.12). The slope derived is no longer significant. From this analysis one may conclude that there is weak evidence for the fact that the slope in the $M_{\rm V} - \log P$-relation is shallower than in the LMC, or, alternatively that there is a change of slope at the short period end. A similar effect is found for the $M_{\rm I} - \log P$-relation (see next section). The implications are discussed further in Sect. 8.

4.2. Zero point of the $M_{\rm I} - \log P$-relation

In Table 2 the zero points of the $M_{\rm I} - \log P$-relation are listed based on V, I photometry. Unless otherwise noted, a slope of -3.05 is used. This is the slope adopted in L99, and is based on work of Tanvir (1999) and Gieren et al. (1998). In every case we have calculated both the zero points for the $M_{\rm I} - \log P$- and $M_{\rm V} - \log P$-relation for the respective samples. For the whole sample we find $\rho = -1.89 \pm 0.11$. This is 0.08 mag brighter than in L99, but within their and our quoted errors. L99 used the magnitude-mean magnitudes in Caldwell & Coulson (1987), and then applied a correction of -0.03 mag to convert these to

Table 1. Values for the zero point from BV photometry.

Solution	N	Zero point in V	Total Weight	Remarks
1	220	-1.403 $\pm$ 0.104	1598.1	FC solution 1 (whole sample)
2	219	-1.399 $\pm$ 0.130	1002.2	FC solution 2 (whole sample minus Polaris)
3	210	-1.427 $\pm$ 0.144	844.9	FC solution 3 (whole sample minus overtones)
4	25	-1.442 $\pm$ 0.154	751.0	FC solution 4 (high weight minus Polaris)
5	20	-1.499 $\pm$ 0.177	595.4	FC solution 5 (high weight minus overtones)
6	26	-1.428 $\pm$ 0.144	1346.9	FC solution 6 (high weight plus Polaris)
7	1	-1.410 $\pm$ 0.170	595.9	FC solution 10 (Polaris)
8	10	-1.377 $\pm$ 0.149	753.2	FC sample, only overtones
9	9	-1.254 $\pm$ 0.308	157.3	FC sample, overtones minus Polaris
10	236	-1.411 $\pm$ 0.100	1718.6	All stars
11	204	-1.492 $\pm$ 0.150	824.5	All fundamental modes
12	32	-1.339 $\pm$ 0.135	894.1	All overtones
13	31	-1.201 $\pm$ 0.219	297.5	All overtone minus Polaris
14	10	-1.417 $\pm$ 0.128	1067.4	$V_{\rm obs} < 5.5$
15	19	-1.461 $\pm$ 0.122	1225.0	$V_0 < 5.5$
16	165	-1.248 $\pm$ 0.095	1656.7	$\pi > 0$, all stars
17	138	-1.154 $\pm$ 0.134	764.2	$\pi > 0$, fundamental modes
18	27	-1.332 $\pm$ 0.134	892.6	$\pi > 0$, overtones
19	208	-1.219 $\pm$ 0.229	275.4	weight < 11
20	17	-1.541 $\pm$ 0.267	272.8	$11 \leq$ weight < 29
21	7	-1.494 $\pm$ 0.252	292.5	$29 \leq$ weight < 70
22	3	-1.401 $\pm$ 0.247	281.3	$70 \leq$ weight < 500
23	235	-1.411 $\pm$ 0.124	1122.1	weight < 500
24	27	-1.478 $\pm$ 0.147	846.7	$11 \leq$weight< 500
25	50	-1.680 $\pm$ 0.274	296.3	$\log P < 0.65$
26	54	-1.251 $\pm$ 0.226	292.9	$0.65 \leq \log P < 0.79$, no Polaris
27	62	-1.572 $\pm$ 0.272	271.6	$0.79 \leq \log P < 0.98$
28	69	-1.165 $\pm$ 0.223	261.3	$0.98 \leq \log P$
29	66	-2.016 $\pm$ 0.412	177.7	$\log P < 0.73$, no δ Cep
30	40	-1.607 $\pm$ 0.376	146.7	$0.73 \leq \log P < 0.85$
31	35	-1.205 $\pm$ 0.323	136.9	$0.85 \leq \log P < 0.99$
32	62	-1.254 $\pm$ 0.250	239.2	$0.99 \leq \log P$
33	66	-2.367 $\pm$ 0.410	247.6	$\delta = -2.22$, $\log P < 0.73$, no δ Cep
34	40	-2.085 $\pm$ 0.376	227.7	$\delta = -2.22$, $0.73 \leq \log P < 0.85$
35	35	-1.730 $\pm$ 0.323	222.7	$\delta = -2.22$, $0.85 \leq \log P < 0.99$
36	62	-1.994 $\pm$ 0.252	446.8	$\delta = -2.22$, $0.99 \leq \log P$
37	204	-2.019 $\pm$ 0.149	1349.2	$\delta = -2.22$, all fundamental modes
38	236	-1.885 $\pm$ 0.100	2662.2	$\delta = -2.22$, all stars
39	47	-1.495 $\pm$ 0.110	1555.4	$\pi_{\rm phot} > 1$ mas, all stars, ZP=-1.411
40	45	-1.481 $\pm$ 0.109	1549.7	$\pi_{\rm phot} > 1$ mas, all stars, ZP=-1.485
41	35	-1.643 $\pm$ 0.177	684.1	$\pi_{\rm phot} > 1$ mas, fundamental modes, ZP=-1.411
42	27	-1.615 $\pm$ 0.181	638.1	$\pi_{\rm phot} > 1$ mas, fundamental modes, ZP=-1.615
43	12	-1.386 $\pm$ 0.139	871.3	$\pi_{\rm phot} > 1$ mas, overtones, ZP=-1.411
44	13	-1.386 $\pm$ 0.139	875.9	$\pi_{\rm phot} > 1$ mas, overtones, ZP=-1.386
45	12	-1.434 $\pm$ 0.123	1160.4	$\pi_{\rm phot} > 1.8$ mas, all stars
46	8	-1.388 $\pm$ 0.199	429.1	$\pi_{\rm phot} > 1.8$ mas, fundamental modes
47	3	-1.444 $\pm$ 0.159	708.1	$\pi_{\rm phot} > 1.8$ mas, overtones
48	236	-1.406 $\pm$ 0.100	1710.7	as (10), V larger by 0.005
49	236	-1.434 $\pm$ 0.100	1755.1	as (10), $B-V$ larger by 0.007
50	236	-1.382 $\pm$ 0.100	1673.2	as (10), $(B-V)_0$ larger by 0.009
51	236	-1.417 $\pm$ 0.100	1727.7	as (10), $R_{\rm V}$ larger by 0.05
52	107	-1.155 $\pm$ 0.181	415.3	All stars with $\log P \geq 0.846$
53	107	-1.816 $\pm$ 0.182	754.5	$\delta = -2.22$, All stars with $\log P \geq 0.846$
54	41	-1.954 $\pm$ 0.114	2213.4	$\pi_{\rm phot} > 1$ mas, $\delta = -2.22$, $\log P > 0.50$
55	42	-1.299 $\pm$ 0.115	1187.4	$\pi_{\rm phot} > 1$ mas, $\delta = -3.04$, $\log P > 0.50$

intensity-mean magnitudes. We use for most stars the intensity-mean magnitudes as calculated in G99 from the original data.

As for the solutions based on BV photometry we find that the zero point using only the fundamental modes is brighter than using only the overtone pulsators, but the difference is now less than 1σ. Polaris again is the star with the highest individual weight. Solutions 6-8 illustrate the effect of LK-bias when selecting stars with positive parallaxes.

4.2.1. Selecting on period

As before, we have split up the sample according to period in bins of approximate equal total weight, for all stars (solutions 9-12, excluding Polaris), and for the fundamental pulsators (solutions 13-16, excluding δ Cep, the fundamental pulsator with the highest individual weight). Again we see that the zero point depends on the period bin chosen, but the effect is not as systematic as in the V-band. In Fig. 5 $10^{0.2\rho}$ is plotted against $\log P$. We have made least-square fits as before and find for the whole sample (α, β) = (0.11 $\pm$ 0.11, 0.331 $\pm$ 0.091), for the 48 stars with an individual weight > 5 (α, β) = (0.101 $\pm$ 0.098, 0.332 $\pm$ 0.079), for all 163 fundamental mode pulsators (α, β) = (0.17 $\pm$ 0.14, 0.26 $\pm$ 0.13), and for the 35 fundamental mode pulsators with a weight > 5 (α, β) = (0.17 $\pm$ 0.12, 0.25 $\pm$ 0.11). The slope is again significant at at most the 1σ level.

Solutions 17-21 give the division in period bins for a slope of the PL-relation of -2.35 for the fundamental mode pulsators (the slope in the PL-relation in V is -2.22). After taking into account the difference in zero points in V, the dependence of the zero point in I on period bin is not significant. The least-square fits give the following results for (α, β): the whole sample ($-0.024\pm$ 0.076, 0.343 $\pm$ 0.065), for the 62 stars with an individual weight > 5 (-0.013 ± 0.077, 0.317 ± 0.069), for all 163 fundamental mode pulsators (0.012 $\pm$ 0.093, 0.294 $\pm$ 0.089), and for the 50 fundamental mode pulsators with a weight > 5 (0.032 ± 0.093, 0.264 ± 0.090). As we found previously, a shallower slope gives rise to a smaller or no dependence of the zero point on period.

4.3. Zero point of the $M_{\rm K} - \log P$-relation

Table 3 lists the results for the zero point of the $M_{\rm K} - \log P$-relation and the zero point for the PL-relations in V and I for the same samples. Unless noted otherwise we have used a slope of $\delta = -3.27$ from Gieren et al. (1998). For the whole sample we find a zero point of -2.61 ± 0.17, but note that the corresponding zero points in the V and I band of this subsample are too bright by about 0.11 magnitude compared to the full samples in V and I, and so the true zero point is probably closer to -2.50. These off-sets indicate biases due to the small number of available measurements in the NIR. This is especially clear when further sub-divisions into smaller samples are made, like a division in period (solutions 9-13). Especially in one bin (solution 10) the result depends very much on one star which was taken out (solution 11). After shifting the zero points in K by an amount such as to make the zero points in V all equal there is no evidence for a dependence of the zero point on period.

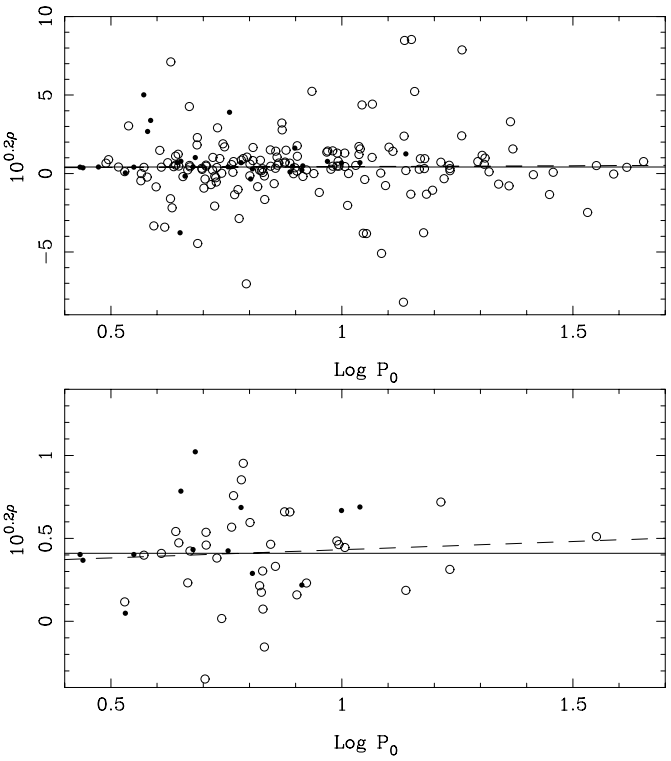

Fig. 5. $10^{0.2\rho}$ versus $\log P$ based on VI colours for a slope of -3.05. In the top panel all 191 stars are plotted. The overtones are marked by the filled symbols. In the bottom panel only the 48 stars with an individual weight > 5 are shown. The solid lines represent the weighted mean of $10^{0.2\rho}$ for the respective samples. The dashed lines represent the weighted least-squares fit to the data for the respective samples.

4.4. Zero point of the $M_{\rm W} - \log P$-relation

Table 4 lists the results for the zero point of the $M_{\rm W} - \log P$-relation. We have used a slope of $\delta = -3.411$ (Tanvir 1999). As before the sample is divided into period bins. After shifting the zero points in W by an amount such as to make the zero points in V all equal (this value can be taken from the corresponding solutions in Table 2) there is no evidence for a dependence of the zero point on period.

5. Summary of the results

5.1. On the use of longer wavelengths

One argument to consider PL-relations in I and K besides the traditional relation in V, is because of the smaller extinction at longer wavelengths. We have calculated the zero points for the whole sample considering a systematic shift for all stars of 0.005 mag in V (respectively I and K), 0.007 in $B-V$ (resp. $V-I$, $J-K$), a shift in the period-colour relations (Eqs. (4), (8), (12)) equal to 1/10-th of the quoted dispersions, and a shift in the selective reddening (Eqs. (5), (10), (14)) equal to the quoted

Table 2. Values for the zero point from VI photometry.

Solution	N	Zero point in I	Total Weight	Zero point in V	Remarks
1	191	-1.892 ± 0.111	2203.4	-1.42 ± 0.10	All stars
2	163	-1.952 ± 0.159	1131.9	-1.49 ± 0.16	All fundamental modes
3	28	-1.830 ± 0.154	1071.5	-1.36 ± 0.14	All overtones
4	1	-1.859 ± 0.204	629.3	-1.41 ± 0.17	Polaris
5	10	-1.889 ± 0.142	1328.4	-1.42 ± 0.13	$V_{\rm obs} < 5.5$
6	139	-1.745 ± 0.105	2137.9	-1.29 ± 0.10	$\pi > 0$, all stars
7	114	-1.671 ± 0.143	1068.9	-1.22 ± 0.14	$\pi > 0$, fundamental modes
8	25	-1.821 ± 0.154	1069.0	-1.35 ± 0.14	$\pi > 0$, overtones
9	35	-1.974 ± 0.270	398.0	-1.51 ± 0.27	$\log P < 0.66$
10	36	-2.039 ± 0.284	383.4	-1.50 ± 0.28	$0.66 \leq \log P < 0.78$, no Polaris
11	44	-2.131 ± 0.286	409.5	-1.61 ± 0.29	$0.78 \leq \log P < 0.92$
12	75	-1.514 ± 0.223	383.2	-1.14 ± 0.22	$\log P \geq 0.92$
13	38	-2.148 ± 0.397	216.6	-1.72 ± 0.40	$\log P < 0.72$
14	35	-2.408 ± 0.451	213.4	-1.99 ± 0.46	$0.72 \leq \log P < 0.85$, no δ Cep
15	29	-1.731 ± 0.351	188.7	-1.21 ± 0.34	$0.85 \leq \log P < 0.99$
16	60	-1.629 ± 0.258	318.7	-1.26 ± 0.25	$\log P \geq 0.99$
17	38	-2.581 ± 0.396	323.7	-2.09 ± 0.40	$\delta = -2.35$, $\log P < 0.72$
18	35	-2.976 ± 0.451	358.9	-2.47 ± 0.46	$\delta = -2.35$, $0.72 \leq \log P < 0.85$, no δ Cep
19	29	-2.349 ± 0.349	335.1	-1.73 ± 0.34	$\delta = -2.35$, $0.85 \leq \log P < 0.99$
20	60	-2.476 ± 0.258	691.6	-2.00 ± 0.25	$\delta = -2.35$, $\log P \geq 0.99$
21	163	-2.571 ± 0.158	2020.5	-2.03 ± 0.16	$\delta = -2.35$, all fundamental modes
22	191	-2.454 ± 0.110	3709.3	-1.90 ± 0.10	$\delta = -2.35$, all stars
23	12	-1.924 ± 0.139	1442.5	-1.43 ± 0.13	$\pi_{\rm phot} > 1.8$ mas, all stars
24	191	-1.887 ± 0.111	2193.3	-1.42 ± 0.10	as (1), I larger by 0.005
25	191	-1.899 ± 0.111	2217.6	-1.42 ± 0.10	as (1), $V-I$ larger by 0.007
26	191	-1.883 ± 0.111	2186.1	-1.42 ± 0.10	as (1), $(V-I)_0$ larger by 0.006
27	191	-1.922 ± 0.111	2262.5	-1.42 ± 0.10	as (1), $R(I)$ larger by 0.19
28	10	-2.469 ± 0.143	2232.3	-1.92 ± 0.13	$\pi_{\rm phot} > 1.8$ mas, $\delta = -2.35$, $\log P > 0.50$
29	11	-1.689 ± 0.144	1082.8	-1.23 ± 0.13	$\pi_{\rm phot} > 1.8$ mas, $\delta = -3.33$, $\log P > 0.50$

Table 3. Values for the zero point from JK photometry.

Solution	N	Zero point in K	Total Weight	Zero point in V	Zero point in I	Remarks
1	63	-2.607 ± 0.169	1821.0	-1.52 ± 0.17	-2.00 ± 0.17	All stars
2	56	-2.645 ± 0.192	1455.6	-1.56 ± 0.19	-2.02 ± 0.20	All fundamental modes
3	7	-2.462 ± 0.353	365.3	-1.41 ± 0.35	-1.94 ± 0.36	All overtones
4	1	-2.692 ± 0.398	355.5	-1.52 ± 0.39	-2.09 ± 0.41	δ Cep
5	6	-2.602 ± 0.227	1006.9	-1.50 ± 0.22	-1.97 ± 0.23	$V_{\rm obs} < 5.5$
6	52	-2.476 ± 0.161	1775.6	-1.39 ± 0.16	-1.87 ± 0.16	$\pi > 0$, all stars
7	45	-2.479 ± 0.181	1410.2	-1.39 ± 0.18	-1.85 ± 0.19	$\pi > 0$, fundamental modes
8	7	-2.462 ± 0.353	365.4	-1.41 ± 0.35	-1.94 ± 0.36	$\pi > 0$, overtones
9	8	-2.601 ± 0.392	337.2	-1.59 ± 0.39	-2.08 ± 0.40	$\log P < 0.64$
10	17	-3.002 ± 0.445	377.9	-1.91 ± 0.45	-2.38 ± 0.45	$0.64 \leq \log P < 0.85$, no δ Cep
11	16	-2.746 ± 0.400	370.4	-1.61 ± 0.40	-2.11 ± 0.40	$0.64 \leq \log P < 0.85$, no δ Cep, no V496 Aql
12	8	-2.833 ± 0.494	262.1	-1.70 ± 0.49	-2.24 ± 0.50	$0.85 \leq \log P < 0.99$
13	29	-2.195 ± 0.270	485.3	-1.18 ± 0.27	-1.50 ± 0.27	$\log P \geq 0.99$
14	3	-2.635 ± 0.271	725.1	-1.49 ± 0.27	-2.01 ± 0.28	$\pi_{\rm phot} > 2.6$ mas, fundamental mode
15	63	-2.599 ± 0.169	1807.9	-1.52 ± 0.17	-2.00 ± 0.17	as (1), K larger by 0.005
16	63	-2.611 ± 0.169	1827.7	-1.52 ± 0.17	-2.00 ± 0.17	as (1), $J-K$ larger by 0.007
17	63	-2.604 ± 0.169	1816.8	-1.52 ± 0.17	-2.00 ± 0.17	as (1), $(J-K)_0$ larger by 0.004
18	63	-2.612 ± 0.169	1830.9	-1.52 ± 0.17	-2.00 ± 0.17	as (1), $R(K)$ larger by 0.097
19	62	-2.800 ± 0.177	1979.3	-2.06 ± 0.18	-2.60 ± 0.18	$\delta = -3.05$, $\log P > 0.5$
20	62	-2.321 ± 0.178	1262.8	-1.31 ± 0.18	-1.74 ± 0.18	$\delta = -3.60$, $\log P > 0.5$

Table 4. Values for the zero point from the Wesenheit-index.

Solution	N	Zero point in W	Total Weight	Remarks
1	191	-2.557 $\pm$ 0.104	4554.1	All stars
2	163	-2.622 $\pm$ 0.156	2167.2	All fundamental modes
3	28	-2.500 $\pm$ 0.141	2387.0	All overtones
4	1	-2.528 $\pm$ 0.176	1555.8	Polaris
5	139	-2.424 $\pm$ 0.100	4431.9	$\pi > 0$, all stars
6	35	-2.626 $\pm$ 0.267	743.3	$\log P < 0.66$, no Polaris
7	36	-2.704 $\pm$ 0.277	737.2	$0.66 \geq \log P < 0.78$
8	44	-2.800 $\pm$ 0.283	771.4	$0.78 \geq \log P < 0.92$
9	75	-2.204 $\pm$ 0.219	746.5	$\log P \geq 0.92$
10	185	-2.558 $\pm$ 0.136	2676.9	$\log P \geq 0.50$
11	12	-2.585 $\pm$ 0.127	3118.8	$\pi_{\rm phot} > 1.8$ mas
12	10	-2.569 $\pm$ 0.134	2808.9	$\pi_{\rm phot} > 1.8$ mas, $\log P \geq 0.50$
13	191	-2.581 $\pm$ 0.104	4656.6	As (1), reddening coefficient of 2.45 in Eq. (11)
14	191	-2.564 $\pm$ 0.104	4584.0	As (1), V larger by 0.005
15	191	-2.545 $\pm$ 0.104	4503.7	As (1), I larger by 0.005

dispersion. The results are listed in Table 1 (solutions 48-51), Table 2 (solutions 23-26), and Table 3 (solutions 15-18). Adding the differences between these zero points and that for the default case in quadrature, one arrives at estimated uncertainties due to errors in the photometry, reddening and period-colour relations of 0.038 mag in V, 0.032 mag in I, and 0.011 mag in K. This illustrates that the K-band PL-relation is indeed the least sensitive to these effects. For the Wesenheit-index the error due to the photometry and reddening coefficients amounts to 0.028 mag (solutions 13-15 in Table 4).

Unfortunately, the advantages of using the infrared, like the intrinsically tighter PL-relation and the insensitivity to reddening, are countered by the fact that so few stars have been measured in the NIR so far. Of the approximately 48 stars with in 1 kpc, BV photometry is available for all of them, VI for 41 of them, but JHK data (of sufficient quality) for only 24. It is estimated that determining the intensity-mean NIR magnitudes of the remaining 24 stars alone would bring the scatter in the zero point determination in the K-band down from about 0.17 to less than 0.1 mag.

5.2. On the slopes of Galactic PL-relations

Another important issue concerns the slopes in the respective Galactic PL-relations. Common practice is to adopt the slope determined for Cepheids in the LMC, but the slope could be different for Galactic Cepheids. In Table 5 we have collected slopes of the PL-relations from the literature for Cepheids in the Galaxy, LMC and SMC, in V, I, K, both observationally determined and from two recent theoretical papers (Alibert et al. 1999, Bono et al. 1999 and private communication). Table 5 includes ths slopes in V and I by Madore & Freedman (1991) used by the HST H_0 Key Project (see for example Gibson et al. 1999). From the results of Gieren et al. (1998) on the Cepheids in the LMC, we have calculated the error in the slope using the data they kindly provided (their Tables 8 and 9). In addition we have calculated the slope and zero point for their data set but using cut-offs in period, for reasons that will be explained later.

There are several interesting features to be noted about the slopes. Observationally, the slopes in the V and I PL-relations in the LMC are very well established, respectively, about -2.81 and -3.05, and these are the default slopes adopted in the present study, with errors of about 0.08 and 0.06. For $M_{\rm K} - \log P$-relation there are fewer observational data available but the slope in Gieren et al. (1998) is determined very accurately and is in reasonable agreement with the result of Madore & Freedman (1991).

One fact needs to be mentioned however, and that is that the period distribution of the calibrating Cepheids in the LMC is very different from that of the Galactic Cepheids in the HIPPARCOS catalog. In Table 8 in Gieren et al. (1998) there are 53 LMC Cepheids listed with V, I photometry that define their PL-relation. Nine have $\log P \leq 0.555$, then there is a gap, and 42 have $\log P \geq 0.846$. In JHK (their Table 9), there are 59 Cepheids, including 5 that have $\log P \leq 0.680$, then there is a gap, and 54 have $\log P \geq 0.834$. The same dichotomy of Cepheids in period can be seen from Tanvir (1999). Note that in more distant Galaxies than the Magellanic Clouds, due to observational bias, most known Cepheids have periods longer than 10 days. We therefore have included in Table 5 the slopes in V, I, K based on the data in Gieren et al. (1998), but have divided the sample according to period. The slopes for the long period subsample differ only slightly from that for the whole sample but are characterised by slightly larger errors. The slopes for the short-period sample have larger errors because of the small number of stars involved but nevertheless are systematically steeper at the 1σ level in all three colours. For comparison, in our sample only 107 of the 236 Cepheids have $\log P \geq 0.846$, and the zero point of this sample differs at the 1.4σ level from that of the whole sample (solution 52 in Table 1). This is yet another indication that for the default slope of -2.81 the zero point may depend

on the period range chosen. For a slope of $\delta = -2.22$ (compare solutions 38, 53) this is not the case.

A second issue concerns the predictions of the theoretical models and the comparison with observations. In V, K for the LMC, and in I for the SMC the models of Bono et al. (1999) are in very good agreement with the observed slope, in I for the LMC and V for the SMC the agreement is poor. In I, K for the LMC, the models of Alibert et al. (1999) are in good agreement with the observed slopes; in V the agreement for the LMC and V, I for the SMC is fair. However, the prediction both models make for the Galaxy are very different. Gieren et al. (1998) have derived PL-relations for Galactic Cepheids using the surface brightness technique. The slopes they find in all three bands are *steeper* than the corresponding slopes in the LMC at the 2-3 σ level. In their paper they ascribe this to small number statistics, and in the end assume the LMC slopes to hold for the Galactic Cepheids as well, also, they add, because the slopes for the LMC Cepheids are better determined. The models of Alibert et al. (1999) predict slopes for the Galactic PL-relations that are *steeper* than the observed ones in the LMC in V, I, K as well, although by a small amount only (the main conclusion of their paper is actually that the slope and zero point of the PL-relations do not depend on metallicity). By contrast, the Bono et al. (1999) paper predicts slopes that are significantly *shallower* in the Galaxy compared to the LMC especially in V, I but also in K. In addition, the Bono et al. models actually predict a non-linear PL-relation in V, for all metallicities considered. Furthermore, Alibert et al. mention that a change of slope in PL-relations is expected at short periods due to the reduction of the blue loop during core He burning, and that this change of slope occurs near $\log P = 0.2$ for Z = 0.004, $\log P = 0.35$ for Z = 0.01, and $\log P = 0.5$ for Z = 0.02. Such a change of slope (in the sense that the slope of the PL-relation is steeper for periods below this limit) was recently observed for SMC Cepheids (Bauer et al. 1999) with the break occurring near $\log P = 0.3$, near the predicted value.

5.3. *Consistency between individual distances based on different colours*

For a given slope and zero point of the PL-relation one can calculate the photometric distance, and since we have determined the zero point for three photometric band we can intercompare photometric distances to individual Cepheids. This is illustrated in Fig. 6, for the default slopes of the PL-relations. The zero point of the $M_{\rm V} - \log P$ relation is fixed at -1.411 (solution 10, Table 1). The zero point of the $M_{\rm I} - \log P$ relation is determined to give a mean difference in $(m-M)_{0,\rm I} - (m-M)_{0,\rm V}$ of zero, and is found to be -1.918 (top panel Fig. 6). The rms dispersion is 0.14 mag. Similarly, to create the bottom panel, the zero point of the $M_{\rm K} - \log P$ relation was determined to give a mean difference in $(m-M)_{0,\rm K} - (m-M)_{0,\rm I}$ of zero, and is found to be -2.600, with an rms dispersion is 0.10. The values for the zero points in I and K derived in this way differ only slightly from the solutions 1 in Tables 2 and 3.

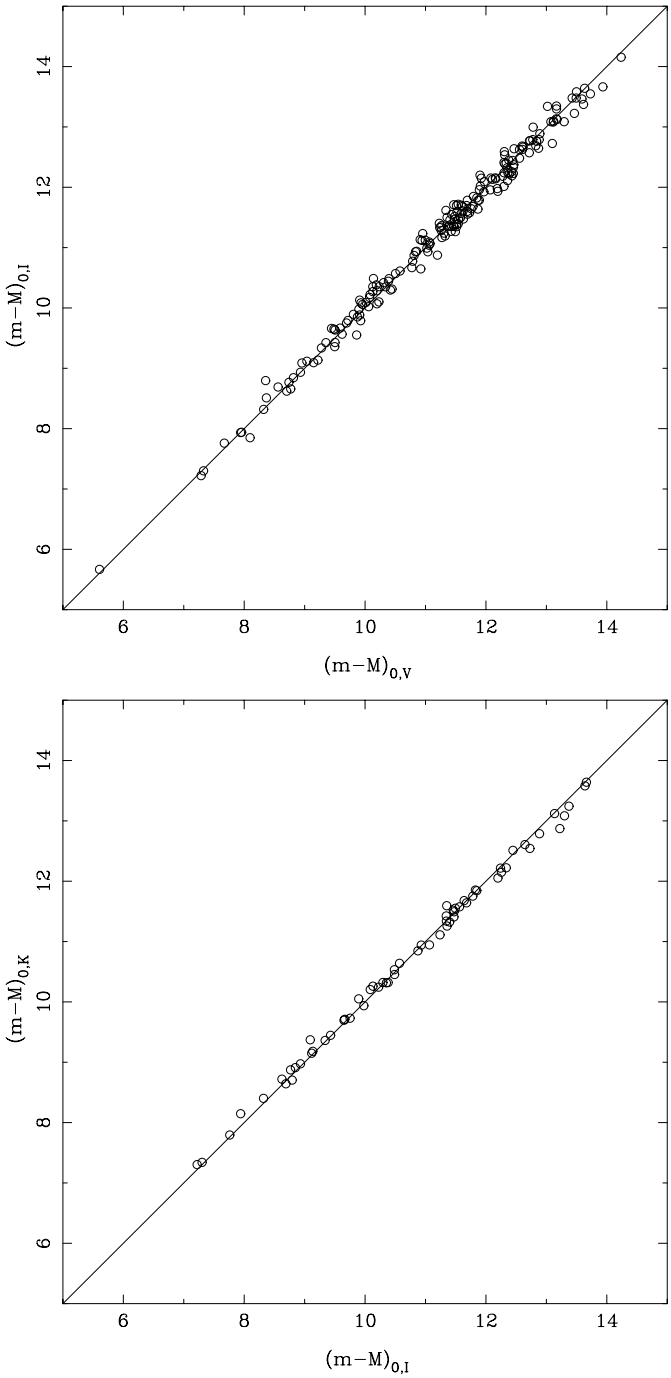

Fig. 6. Comparison of the distance moduli based on the PL-relations in V and I (top panel), assuming zero points of respectively -1.411 and -1.918, and the default slopes, and I and K (bottom panel) for zero points of -1.918 and -2.600, and the default slopes. The solid line is the one-to-one relation, although a least-square fit indicates that the best fitting slope differs slightly from unity (see text).

Interestingly, least-square fitting shows that the slopes of the relations are not unity, but 0.980 $\pm$ 0.007 (top panel), and 0.965 $\pm$ 0.007 (bottom panel). Using the same procedure, but adopting steeper slopes of -3.04, -3.33, -3.60 (see Sect. 8 for the reason of these choices) in, respectively, the $M_{\rm V} - \log P$,

Table 5. Slopes of the PL-relations.

Slope	Colour	System	Reference
-3.037 ± 0.138	V	GAL	Gieren et al. (1998)
-2.22 ± 0.04	V	0.02	Bono et al. (1999); non-linear, $\log P < 1.4$
-2.905	V	0.02	Alibert et al. (1999)
-2.810 ± 0.082	V	LMC	Tanvir (1999)
-2.769 ± 0.073	V	LMC	Gieren et al. (1998)
-2.820 ± 0.118	V	LMC	this work; 44 stars with $\log P > 0.845$ from Gieren et al. (1998)
-3.54 ± 0.68	V	LMC	this work; 9 stars with $\log P < 0.845$ from Gieren et al. (1998)
-2.88 ± 0.20	V	LMC	Madore & Freedman (1991)
-2.81 ± 0.06	V	LMC	Caldwell & Laney (1991)
-2.79 ± 0.06	V	0.008	Bono et al. (1999); non-linear, $\log P < 1.4$
-2.951	V	0.01	Alibert et al. (1999)
-2.63 ± 0.08	V	SMC	Caldwell & Laney (1991),
-3.04 ± 0.04	V	0.004	Bono et al. (1999); non-linear, $\log P < 1.4$
-2.939	V	0.004	Alibert et al. (1999)
-3.329 ± 0.132	I	GAL	Gieren et al. (1998)
-2.35 ± 0.08	I	0.02	Bono et al. (1999)
-3.102	I	0.02	Alibert et al. (1999)
-3.078 ± 0.059	I	LMC	Tanvir (1999)
-3.041 ± 0.054	I	LMC	Gieren et al. (1998)
-3.084 ± 0.088	I	LMC	this work; 44 stars with $\log P > 0.845$ from Gieren et al. (1998)
-3.39 ± 0.39	I	LMC	this work; 9 stars with $\log P < 0.845$ from Gieren et al. (1998)
-3.14 ± 0.17	I	LMC	Madore & Freedman (1991)
-3.01 ± 0.05	I	LMC	Caldwell & Laney (1991)
-2.63 ± 0.08	I	0.008	Bono et al. (1999)
-3.140	I	0.01	Alibert et al. (1999)
-2.92 ± 0.07	I	SMC	Caldwell & Laney (1991)
-2.73 ± 0.10	I	0.004	Bono et al. (1999)
-3.124	I	0.004	Alibert et al. (1999)
-3.598 ± 0.114	K	GAL	Gieren et al. (1998)
-3.03 ± 0.07	K	0.02	Bono et al. (1999)
-3.367	K	0.02	Alibert et al. (1999)
-3.267 ± 0.041	K	LMC	Gieren et al. (1998)
-3.304 ± 0.052	K	LMC	this work; 54 stars with $\log P > 0.833$ from Gieren et al. (1998)
-3.37 ± 0.39	K	LMC	this work; 5 stars with $\log P < 0.833$ from Gieren et al. (1998)
-3.42 ± 0.09	K	LMC	Madore & Freedman (1991)
-3.19 ± 0.09	K	0.008	Bono et al. (1999)
-3.395	K	0.01	Alibert et al. (1999)
-3.27 ± 0.09	K	0.004	Bono et al. (1999)
-3.369	K	0.004	Alibert et al. (1999)
-3.411 ± 0.036	Wesenheit	LMC	Tanvir (1999)

$M_{\rm I} - \log P$ and $M_{\rm K} - \log P$ relations and fixing the zero point of the $M_{\rm V} - \log P$ relation at -1.234 we find in the same way the zero points of the $M_{\rm I} - \log P$ and $M_{\rm K} - \log P$-relations to be -1.696 and -2.328. The slopes are 0.983 $\pm$ 0.007 and 0.971 $\pm$ 0.007.

Using the same procedure, but adopting shallower slopes of -2.22, -2.35, -3.05 in, respectively, the $M_{\rm V} - \log P$, $M_{\rm I} - \log P$ and $M_{\rm K} - \log P$ relations and fixing the zero point of the $M_{\rm V} - \log P$ relation at -1.885 (solution 38 in Table 1) we find the zero point of the $M_{\rm I} - \log P$ and $M_{\rm K} - \log P$-relations to be -2.491 and -2.692. The slopes are 0.974 $\pm$ 0.007 and 1.010 $\pm$ 0.010.

The conclusion is the the photometric distances based on different PL-relations are consistent with each other at a level of 0.10-0.14 mag, similar to the uncertainties in the individually derived zero points in V, I, K for the full sample. The data does not allow to discriminate between different choices of the slopes of the PL-relations.

6. A volume complete sample

The question remains how representative the HIPPARCOS Cepheid sample is. As with all stars that made it in the HIPPARCOS catalog, they were proposed by Principal Investigators in solicited proposals. If proposers preferred their 'favorite' objects to be observed, there may be a 'Human' bias, which is impossible to correct for. For example, at some point in the selection process of the HIPPARCOS Input Catalog the number of

Cepheids with magnitudes between 9.5 and 11 were 'tuned-up' (ESA 1989, page 80). Also, the distribution in pulsation period of the about 72 Cepheids that were proposed to be observed but did not end up in the HIPPARCOS Input Catalog is somewhat different from the 270 that did make it (ESA 1989, page 96).

In view of this it may be instructive to try to construct a volume complete sample. The HIPPARCOS Input Catalog (ESA 1989, page 94) mentions that *all* 55 Cepheids within 1 kpc have been included. This depends of course on the adopted slope and zero point to calculate the photometric parallax. The F95 database lists 51 stars within 1 kpc for their adopted relation of $M_{\rm V} = -2.902\ \log P - 1.203$.

In Fig. 7 the cumulative (photometric) parallax distribution is plotted for the 236 stars in the sample, with distances from F95, or calculated in the same way for the stars not listed there. Also indicated is a line with slope -2 as expected for a disk population (with $N(r)dr \sim r$ it follows that $N(\pi)d\pi \sim \pi^{-3}$, and so the cumulative distribution is proportional to π^{-2}). From this figure it is confirmed that the HIPPARCOS catalog is volume complete to approximately 1 kpc.

On the other hand, three new Cepheids were discovered with HIPPARCOS. For the same slope and zero point as used in F95 the photometric parallaxes of CK Cam, V898 Cen, V411 Lac are 1.77, 0.73 and 1.17 mas, respectively.

As HIPPARCOS discovered 2 Cepheids that are closer than 1 kpc, it implies that the present sample may now be indeed complete down to 1 mas, but is possibly only complete for stars with a parallax $\gtrsim$1.8 mas as no new Cepheids closer than this limit have been discovered.

In Tables 1-4 we include solutions for volume complete samples, or, in other words, complete in photometric parallax. Since this depends on the zero point itself, this is an iterative process. For the $M_{\rm V} - \log P$-relation we give the results in Table 1 for a cut-off at 1 and 1.8 mas. In solutions 39, 41, 43 we list the zero point for an input zero point of -1.411 (solution 10) for the whole sample, the fundamental pulsators, and the overtones, respectively. The next line (solutions 40, 42, 44) lists the final result after iteration on the zero point. Solutions 45-47 give the final results for a higher cut-off in photometric parallax. In most cases the zero points are slightly brighter than the corresponding solutions 10, 11, 12. This is a bit surprising because of the Malmquist bias one expects the volume complete sample to be dimmer. The expected Malmquist bias for a disk population with an intrinsic spread of $\sigma_{\rm H}$ = 0.10 around the mean is about 0.009 mag (Stobie et al. 1989). This is much smaller than the typical error estimate in the zero points, and so the fact that the volume complete sample is brighter probably reflects the slightly different nature of that sample. For example, the mean value of $\log P_0$ for the whole sample is 0.86, while that for the volume complete sample is 0.77. As we noticed earlier, since the shortest period bins give brighter zero points this could be an explanation.

For the $M_{\rm I} - \log P$-relation the construction of a volume complete sample is slightly more complicated due to the fact that for some of the 47 stars with BV photometry and a photometric parallax > 1 mas no I-band photometry is available.

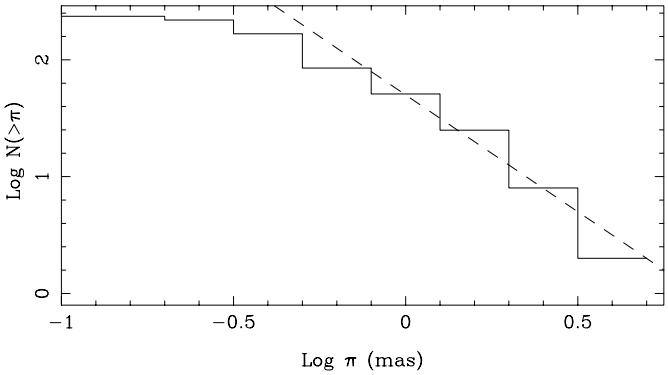

Fig. 7. Cumulative (photometric) parallax distribution of the 236 stars in the sample with distances from F95 who calculated them using $M_{\rm V} = -2.902\ \log P - 1.203$. The dashed line has a slope of -2, as expected for a disk population. It shows that HIPPARCOS is volume complete down to a distance of about 1 kpc.

This implies that one has to apply a more stringent criterion to obtain a volume complete sample of stars that also have I-band photometry. This turns out to be a photometric parallax limit of 1.8 mas, and solution 23 lists the result. The zero point is slightly brighter, and this again may be due to the fact that the average $\log P_0$ value is smaller (0.74) than for the whole sample (0.90).

In the K-band no meaningful volume complete sample can be constructed. As there is no NIR data available for Polaris, any volume complete sample could be constructed for fundamental pulsators only. In any case, even then, a volume complete sample of stars with NIR data would have a cut-off at 2.6 mas, and would only include 3 stars. For completeness, it has been included in Table 3 (sol. 14).

The conclusion is that the zero point of the PL-relation based on a volume complete sample are within 1σ of the results for the full sample. Surprisingly, the zero points are brighter, contrary to one would expect from Malmquist bias. However, the Malmquist correction is expected to be small (see the next section for an estimate based on numerical simulations), and certainly much smaller than the error in the zero point, so that this effect is due to the slightly different nature of the volume complete samples compared to the full samples.

7. Properties of the HIPPARCOS Cepheids, and numerical simulations

In this section we describe a numerical model to first of all construct synthetic samples of stars that fit some observed properties of the HIPPARCOS Cepheids. Second, this model is used to investigate the numerical bias involved in applying the "reduced parallax" method.

The observed distributions of the fundamental period, the V magnitude, de-reddened $(B-V)_0$, colour excess, and absolute distance to the Galactic plane are plotted in Fig. 8 for the 236 Cepheids in our sample (the dotted lines). For the overtones, the fundamental period was calculated following Eqs. (6-7). $(B-V)_0$ follows from Eq. (4), and $E(B-V)$ from the

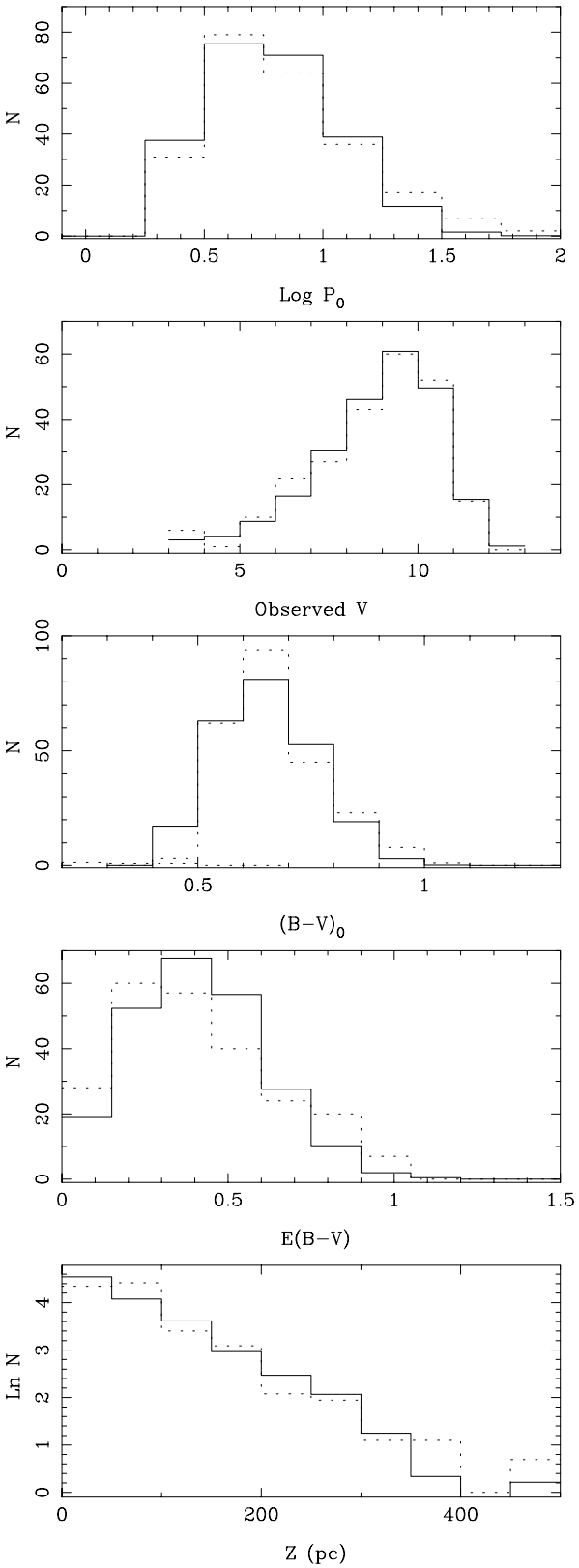

Fig. 8. Observed (dotted line) and numerical simulation (solid line) of the 236 Cepheids in HIPPARCOS. Harmonic periods have been converted to the fundamental period. For a description of the model, and the parameters see Sect. 6.

observed value of $(B-V)$ minus $(B-V)_0$. The absolute distance to the Galactic plane is calculated from the galactic latitude combined with the de-reddened V-magnitude and a photometric distance based on Eq. (1) with $\delta = -2.81$ and $\rho = -1.43$. The distributions are compared to simulations described now.

We have devised a numerical code to simulate the distributions described above. The input period distribution is (assumed ad-hoc to be) a Gaussian in $\log P$ with mean $X_{\rm P}$, and spread $X_{\sigma \rm P}$. Based on the observed properties of the sample only $\log P$ values between 0.43 and 1.66 are allowed. A random number is drawn and a $\log P$ selected following this distribution. The values of $X_{\rm P}$ and $X_{\sigma \rm P}$ directly influence the resulting distribution and so are easily determined. We find that values of $X_{\rm P}$ between 0.65 and 0.75 and of $X_{\sigma \rm P}$ between 0.2 and 0.25 give acceptable fits.

The galactic distribution of Cepheids is assumed to be a double exponential disk with a scale height H in the z-direction (the coordinate perpendicular to the galactic plane), and a scale height $R_{\rm GC}$ in the galacto-centric direction. The coordinate system used is cylindrical coordinates centered on the Galactic Centre. Three random numbers are drawn to select the distance to the Galactic plane, the distance to the Galactic centre and a random angle ϕ between 0 and 2π in the Galactic plane centered on the Galactic centre. From this the distance d to the Sun is calculated. Based on the observed photometric parallaxes of the sample only stars closer than 7800 pc to the Sun are allowed. We find no evidence for a gradient in the number of Cepheids with galacto-centric radius, in other words $R_{\rm GC} = \infty$ gives good fits, probably indicating that the volume sampled is too small to detect such a gradient, or that the distribution of Cepheids is at least equally determined by another factor, for example the location of the spiral arms. The value of H is directly determined by the distribution of the number of stars as a function of z, and is found to be between 60 and 80 pc. This is consistent with the scale height of a relative massive population of stars, as the Cepheids are.

The value of $M_{\rm V}$ and $(B-V)_0$ are correlated in the sense that brighter Cepheids are also bluer for a given period. Contrary to other studies we do not assume a Gaussian spread around the $M_{\rm V} - \log P$ and $(B-V)_0 - \log P$ relations, but instead a 'box' like distribution which is more physical because of the finite width of the instability strip. However, this does assume that the instability strip is uniformly filled (for all periods).

A single uniform random number, Rn, is drawn and then

$$M_{\rm V} = -2.81\ \log P - 1.43 + \ (-0.42 + 0.84 \times {\rm Rn}) \qquad (15)$$

and

$$(B-V)_0 = 0.416 \log P + 0.314 + (-0.15 + 0.3 \times {\rm Rn}) \qquad (16)$$

are calculated. The full width of the instability strip in $M_{\rm V}$ is taken to be 0.84 magnitude (derived from plots in Gieren et al. 1998, Tanvir 1999), and that of the $(B-V)_0$ relation to be 0.3 mag. (Laney & Stobie 1994).

The reddening is calculated from:

$$A_{\rm V} = 0.09\ \frac{1 - \exp\left(-0.0111\ d\ \sin b\right)}{\sin b} \qquad (17)$$

where b is the absolute value of the galactic latitude. The colour excess is then calculated using Eq. (5). The factor in front was varied to fit the $E(B-V)$ distribution. We also tried the reddening model of Arenou et al. (1992), but found that it could not fit the $E(B-V)$ distribution.

The simulated 'observed' visual magnitude is calculated from $V = M_{\rm V} + 5\ \log d - 5 + A_{\rm V}$. Then a term is added simulating the uncertainty in the observed V, which is described by a Gaussian distribution with a dispersion of 0.005 mag.

HIPPARCOS was complete only down to about $V = 7$ and the following function was used to determine if a star was 'observed' or not. A random number (Rn) was drawn to calculate:

$$V_{\rm lim} = 7.0 - \frac{\log(1.0 - {\rm Rn})}{C} \tag{18}$$

with C empirically determined to be:

$$C = 0.107 - 0.030\ y - 0.00482\ y^2 + 0.00361\ y^3 \tag{19}$$

with $y = (V-7)$. A star is 'observed' if $V < V_{\rm lim}$.

The simulation is continued until 25 sets of 236 stars fulfill all criteria. Typically 100 000 stars needed to be drawn to arrive at this. The simulated distributions are depicted in Fig. 8 using the solid lines (normalised to the observed number of 236 stars). Typical parameters $X_{\rm P} = 0.70$, $X_{\sigma{\rm P}} = 0.25$, and $H = 70$ pc have been used. The overall fit is good.

This numerical code for the quoted parameters provides us with a tool with which synthetic samples of Cepheids can be generated that obey the observed distributions.

The main difference with the simulations of L99 is in the conclusion about the space distribution of Cepheids. They assume a homogeneous 3D distribution, and consider a box centered on the Sun of 4200 pc on a side. They justify this because of "the relative small depth of the HIPPARCOS survey [with respect to] the depth of the Galactic disk". This is not true however. First of all, using any reasonable combination of δ and ρ it is clear that HIPPARCOS sampled Cepheids to much greater distances than 2.1 kpc, in fact out to 7-8 kpc. Furthermore, since the scale height of 3-10 $M_\odot$ main-sequence stars (the progenitors of the Cepheids variables) is of order 100 pc it is clear that HIPPARCOS sampled to distances much larger than the scale height of the Cepheid population. This is directly confirmed from our simulations from which we derive a scale height of about 70 pc. In other words, the space distribution of the Cepheids is a disk population, not a homogeneous population.

This might have consequences for the results of the L99 paper concerning biases which are difficult to judge by us. Another consequence is related to the fact that both Malmquist- and LK-bias depend on the underlying distribution of stars. For example, Oudmaijer et al. (1998) calculated the LK-bias assuming a homogeneous distribution of Cepheids. For a disk population the values of both the Malmquist- and LK-bias are smaller (Stobie et al. 1989, Koen 1992).

Now, we will discuss whether the zero points derived by the method outlined in Sect. 4 are subject to bias or not. Similar simulations were also performed by L99 and Pont (1999). L99 concluded that zero points derived for the whole sample in V are too bright by 0.01 mag. Pont (1999) concluded that any bias is less than 0.03 mag.

What remains to be discussed in relation to our numerical model is how the 'observed' parallax and the error in the parallax are calculated.

We define several quantities. First of all a minimum error in the parallax, calculated from (in mas):

$$\begin{aligned} \sigma_\pi^{\rm min} &= 0.45 & V \le 8 \\ &= 0.45 \times (V/8)^{3.2} & \text{else} \end{aligned} \tag{20}$$

Second of all, an error in the error on the parallax, calculated from (in mas):

$$\begin{aligned} \sigma_\sigma &= 0.18 & V \le 8 \\ &= 0.18 - 0.2167\,y + 0.325\,y^2 - 0.06833\,y^3 & \text{else} \end{aligned} \tag{21}$$

with $y = (V-8)$. Third, a 'mean' error on the parallax, calculated from (in mas):

$$\begin{aligned} \sigma =& 0.80 & V \le 5 \\ =& 0.80 - 0.0280y - 0.00229y^2 + 0.008651y^3 & \text{else} \end{aligned} \tag{22}$$

with $y = (V-5)$. All fits have been made with IDL using the routine POLYFIT from the full sample of 236 stars. It was verified that the synthetic samples have the same distribution of parallax and parallax error compared to the observed sample.

The error on the parallax, σ_π, was then determined from σ plus a quantity randomly selected from a Gaussian distribution with dispersion σ_σ. The result is only accepted when $\sigma_\pi > \sigma_\pi^{\rm min}$ however. Finally, the 'observed' parallax (in mas) is calculated from 1000/d, with d the true distance in pc, plus a quantity randomly selected from a Gaussian distribution with dispersion σ_π.

The simulation is continued until 100 sets of 236, 191, or 63 stars fulfill all criteria, depending whether the simulation relates to V, I or K. About 410 000 stars have to been drawn to arrive at 23 600 'observed' stars in V. This was done with the parameter set that best described the observed distributions, as discussed above, i.e. with $X_{\rm P} = 0.70$, $X_{\sigma{\rm P}} = 0.25$, and $H = 70$ pc.

In the case the simulation relates to I and K the procedure is as follows. First the stars are selected according to the procedure outlined above, that is, selection based on V-photometry. For the stars that fulfill the criteria, the 'observed' $I, V-I$ (respectively K, $J-K$) colours are determined, using the period-colour and reddening relations outlined in Sect. 4. The *same random number* that was used in Eqs. (15-16) to calculate the true $M_{\rm V}$ and $(B-V)$ is used to calculate $M_{\rm I}$ and $(V-I)$, respectively $M_{\rm K}$ and $(J-K)$. This is to simulate the fact that if the synthetic star is 'observed' to be fainter and bluer than the mean in V, this is also the case at other wavelengths. This procedure ignores any phase shifts between the light curves at different colours. For the full-width of the instability strip (cf. Eqs. (15-16)) in $M_{\rm I}$ we take 0.70 mag, in $(V-I)$ 0.20 mag, in $M_{\rm K}$ 0.60 and in $(J-K)$ 0.16 mag (Gieren et al. 1998).

For every set of 236, 191, or 63 stars we apply the "reduced parallax" method and derive the zero point. From the distribution of the zero points of the 100 sets, we determine the mean, and the dispersion. The results are given in Table 6, where we

list the zero point assumed in the numerical simulation, the zero point retrieved, the average number of stars in the simulation that fulfilled the selection criteria, and to which solution the simulation refers to. From the results we see that the zero point of the volume complete sample is dimmer than for the whole sample, as expected from Malmquist bias. In any case, the biases are very small, of order 0.01 mag, or less, similar to the results found by L99 and Pont (1999). Second, we confirm the result by Pont (1999) that the errors derived are somewhat larger compared to the outcome of the "reduced parallax" method. However the differences are not so large as compared to the error bars quoted in FC.

From the simulations we find that the smallest error is for the sample selected on parallax (as was found for the 'real' sample), but that it is subject to Lutz-Kelker bias.

8. Discussion

8.1. The finally adopted zero points

Based on the results obtained in Sects. 4, 5 and 6, we will present three sets of solutions, a 'traditional' one, and two alternatives. The traditional one follows FC and L99 closely. The zero point adopted is the one for the entire sample (which has the lowest error of the samples that are not selected on observed parallax), adopting the slope of the PL-relation observed for Cepheids in the LMC. This would then be solution 10 from Table 1 ($\rho = -1.41 \pm 0.10$), solution 1 from Table 2 ($\rho = -1.89 \pm 0.11$) and solution 1 from Table 3 corrected for the off-set in the corresponding solution in V and I as discussed in Sect. 4.3 ($\rho = -2.50 \pm 0.17$). These zero points have to be corrected for Malmquist bias. If the Malmquist bias would be evaluated in magnitude space, this bias would amount to 0.0092, 0.021 and 0.013 magnitude in V, I, K, respectively, for a disk population and the adopted values for $\sigma_{\rm H}$ of, respectively, 0.10, 0.15 and 0.12 mag (Stobie et al. 1989). However, if evaluated using the reduced parallax method the Malmquist bias is smaller (see Oudmaijer et al. 1999), and from the numerical simulations (Table 6) we find a Malmquist bias of 0.007 in V, 0.003 in I, and an unphysical negative value in K, probably due to the smaller number of stars involved. For the Malmquist bias we will assume a (round number) of 0.01 mag in all three bands.

Also, we have increased the errors in the zero points to reflect the sensitivity to uncertainties in the photometry, reddening and period-colour relations (see Sect. 5.1). For adopted slopes of -2.81, -3.05 and -3.27, the finally adopted zero points of the PL-relations in V, I and K are, respectively, $\rho = -1.40 \pm 0.11$, -1.88 ± 0.12 and -2.49 ± 0.17. For the Wesenheit-index, after correcting for Malmquist bias and increasing the error bar due to the uncertainties described in Sect. 5.1, we adopt a zero point of -2.55 ± 0.11 for a slope of -3.411.

The 'traditional' solution above has certain advantages, like the fact that the errors are smallest compared to solutions that do not include all stars, or, since the slope adopted is the one in the LMC, a distance determination to the LMC is essentially a comparison of zero points only (apart from systematic effects). On the other hand, alternative solutions can be presented which also have merits. These solutions are based on a volume complete sample (at least in V and I) to avoid Malmquist bias. Although small, its value does depend on the distribution of stars, and the intrinsic spread in the PL-relation and selecting a volume complete sample avoids Malmquist bias outright. In K, no volume complete sample could be constructed and we used the full sample instead. The alternative solutions take into account the theoretical prediction that the slope of the PL-relation may change at $\log P \sim 0.5$ for solar metallicities (Alibert et al. 1999). Where the two alternative solutions differ are in the adopted slopes for the Galactic PL-relations. One alternative solution takes into account the, admittedly at the 1σ level of significance, evidence presented in Sects. 4.1-4.2 that the slope of the Galactic PL-relations are shallower than the ones in the LMC, and in accordance we have adopted the theoretical slopes predicted by Bono et al. (1999) for solar metallicities. The second alternative method adopts the slopes in Gieren et al. (1998), who derived distances from the infrared version of the surface brightness technique to Galactic Cepheids, which yields steeper slopes than for the LMC.

These alternative solutions are presented in Tables 1-3 (solutions 54-55, 28-28 and 19-20, respectively). The zero points in K have to be corrected for Malmquist bias (+0.01 mag) and for the off-sets in the corresponding V and I solutions, and the errors in all three zero points are increased for reasons indicated above. For the adopted slopes of -2.22, -2.35 and -3.05, the zero points of the PL-relations in V, I and K are, respectively, $\rho = -1.95 \pm 0.12$, -2.47 ± 0.15 and -2.68 ± 0.18. For the adopted slopes of -3.04, -3.33 and -3.60, the zero points of the PL-relations in V, I and K are, respectively, $\rho = -1.30 \pm 0.13$, -1.75 ± 0.14 and -2.30 ± 0.18.

8.2. PL-relation of LMC Cepheids

Before proceeding we have to adopt PL-relations for the LMC Cepheids. In V, for a slope of -2.81, Caldwell & Laney (1991) find a zero point of 17.23 $\pm$ 0.02. Tanvir (1999), for the same slope, gives an observed zero point of 17.451 $\pm$ 0.043. Adopting a mean reddening to the LMC of $E(B-V)$ of 0.08 (Caldwell & Laney 1991) and a ratio of total-to-selective reddening of $R_{\rm V} = A_{\rm V}/E(B-V) = 3.27$ (Eq. (5) for typical colors) we derive a de-reddened zero point of 17.19 $\pm$ 0.04. For the Cepheids in the LMC we adopt the weighted mean of these two values, or a zero point of 17.22 $\pm$ 0.02 in V for a slope of -2.81.

In I, for a slope of -3.041, Gieren et al. (1998) find a zero point of 16.74 $\pm$ 0.06 (the error is calculated by us, from their data). Tanvir (1999), for a slope of -3.078, gives an observed zero point of 16.904 $\pm$ 0.031. Adopting $A_{\rm I} = 0.69 A_{\rm V} = 0.18$ mag for the reddening in V calculated as above, we derive a zero point of 16.72 $\pm$ 0.03. For the default slope of -3.05 we adopt the weighted mean of these two values, or a de-reddened zero point in the I band for the Cepheids in the LMC of 16.72 $\pm$ 0.02.

In K, for a slope of -3.267, Gieren et al. (1998) find a zero point of 16.03 $\pm$ 0.05 (the error is calculated by us from their data) for the Cepheids in the LMC. This value is adopted by us.

Table 6. Zero points from numerical simulations.

Input	Result	Number	Band	Remarks
-1.43	-1.425 ± 0.124	236	V	all stars, solution 10
-1.43	-1.418 ± 0.140	33	V	volume complete sample, solution 39
-1.43	-1.431 ± 0.175	11	V	$V_{\rm obs} < 5.5$, solution 14
-1.43	-1.197 ± 0.114	165	V	$\pi > 0$, solution 16
-1.43	-1.457 ± 0.241	215	V	weight < 11, solution 19
-1.43	-1.421 ± 0.289	13.3	V	$11 <$ weight < 29, solution 20
-1.43	-1.443 ± 0.327	4.8	V	$29 <$ weight < 70, solution 21
-1.43	-1.400 ± 0.259	2.4	V	$70 <$ weight < 500, solution 22
-1.43	-1.425 ± 0.130	236	V	weight < 500, solution 23
-1.43	-1.416 ± 0.157	20	V	$11 <$ weight < 500, solution 24
-1.90	-1.907 ± 0.143	191	I	all stars, solution 1
-1.90	-1.904 ± 0.206	8.5	I	volume complete sample, solution 22
-1.90	-1.664 ± 0.131	134	I	$\pi > 0$, solution 6
-2.60	-2.610 ± 0.261	63	K	all stars, solution 1
-2.60	-2.617 ± 0.435	1.3	K	volume complete sample, solution 14
-2.60	-2.339 ± 0.234	45	K	$\pi > 0$, solution 6

Table 7. Metallicity dependence of the absolute magnitude between Galaxy and LMC from recent theoretical models.

$\log P_0$	$\Delta M_{\rm V}$	$\Delta M_{\rm I}$	$\Delta M_{\rm K}$	Reference
0.77	0.139	0.145	0.073	Bono et al. (1999)
0.77	0.005	-0.007	0.004	Alibert et al. (1999)
0.47	-0.032	0.062	0.025	Bono et al. (1999)
0.47	-0.008	-0.018	-0.003	Alibert et al. (1999)

For the Wesenheit-index, for a slope of -3.411, Tanvir (1999) finds a zero point of 16.051 $\pm$ 0.017. This value is adopted by us.

8.3. Metallicity correction

We will now consider the effect of metallicity on the zero point. For comparison, FC applied a correction of +0.042 mag to the zero point in the V-band, based on Laney & Stobie (1994). The theoretical models of Bono et al. (1999), and Alibert et al. (1999) provide PL-relations and from those the difference $\Delta M = M$(Gal) $-M$(LMC) can be determined which will depend on the photometric band and period. We have determined this difference for two periods, namely for $\log P_0 = 0.77$ which we have determined to be the mean period of the volume complete sample of Galactic Cepheids in HIPPARCOS and for $\log P_0 = 0.47$ which is the mean period of Cepheids in the LMC (Alcock et al. 1999). The results for ΔM are listed in Table 7 for the three photometric bands. This illustrates the difference between the two theoretical models, for the Alibert et al. (1999) models predict essentially no dependence on metallicity, while the Bono et al. (1999) models predict a significant metallicity dependence, which mostly is in the sense that the metal-rich pulsators are fainter than the metal-poor ones. This is at variance with various empirical estimates that give the opposite result, and that, in the V-band, vary between -0.24 ± 0.16 (Kennicutt et al. 1998) and about -0.4 mag/dex (Kochanek 1997, Sasselov et al. 1997, Storm et al. 1999[2]). A mean of these four determinations is -0.38 ± 0.09 mag/dex, which for a difference in metallicity of 0.4 dex, implies $\Delta M = -0.15 \pm 0.04$ in the V-band. In the I-band we assume the same value following Sasselov et al. (1997) and Kochanek (1997), but the reader should realise that this number is less well established than the correction in V, and in the K-band adopt $\Delta M = -0.07$. Note however, that a metallicity dependence as large as 0.4 mag in V as suggested by Sekiguchi & Fukugita (1998) can be excluded at the 6σ level (Laney 1999, 2000). In recent papers, Saio & Gautschy (1998) and Sandage et al. (1999) found no significant metallicity dependence on the bolometric PL-relation, and slopes of -0.08 mag/dex in V and -0.1 mag/dex in I (Sandage et al. 1999), which represents a shallower dependence than the values listed above, that are adopted in the present study, and which therefore may be an extreme view.

8.4. The distance to the LMC

In Table 8 are listed the true distance moduli (DM) to the LMC for V, I, K, the three slopes ('traditional' meaning the observed slopes for the Cepheids in the LMC, 'shallower' adopting the theoretical slopes from Bono et al. and 'steeper' adopting the observed slopes for Galactic Cepheids from Gieren et al. (1998) and the three metallicity corrections ('0' means no correction, '+' means a longer distance scale as implied by the models from Bono et al., and '$-$' means a shorter distance scale as implied from empirical evidence). The error quoted includes the error

[2] Recently, Storm (2000) suggested that this result may not be confirmed from his latest analysis and that the correction may have a positive sign instead.

Table 8. Distance Moduli to the LMC. Based on the PL-relations in V, I, K and the Wesenheit-index, for different assumptions about the slope of the Galactic PL-relation, and metallicity correction.

Solution	Slope	Metallicity dependence	V	I	K	W	Mean over V, I, K
1	traditional	0	18.62 ± 0.11	18.60 ± 0.12	18.52 ± 0.18	18.60 ± 0.11	18.60 ± 0.07
2	traditional	+	18.71 ± 0.12	18.70 ± 0.13	18.57 ± 0.18		18.68 ± 0.08
3	traditional	−	18.47 ± 0.12	18.45 ± 0.12	18.45 ± 0.18		18.46 ± 0.08
4	shallower	0	18.80 ± 0.14	18.76 ± 0.19	18.57 ± 0.19		18.73 ± 0.10
5	shallower	+	18.86 ± 0.12	18.86 ± 0.16	18.62 ± 0.19		18.81 ± 0.09
6	shallower	−	18.65 ± 0.14	18.61 ± 0.18	18.50 ± 0.19		18.60 ± 0.10
7	steeper	0	18.66 ± 0.13	18.64 ± 0.15	18.53 ± 0.19		18.63 ± 0.09
8	steeper	+	18.72 ± 0.18	18.75 ± 0.16	18.58 ± 0.20		18.70 ± 0.10
9	steeper	−	18.51 ± 0.14	18.49 ± 0.15	18.46 ± 0.19		18.49 ± 0.09
mean/range			18.67 / 0.20	18.65 / 0.21	18.53 / 0.09		18.63

in the zero point of both the Galactic and LMC Cepheids, and where appropriate, the error due to the metallicity correction, and for the solutions with either steeper or shallower slope, the uncertainty due to the difference in DM at $\log P = 0.47$ and 0.77.

Also included are the weighted mean DM, averaged over V, I, K (with internal error), and, for reference, the (unweighted) mean DM per photometric band of all the solutions (with the one-sided range in the solutions). Also included is the solution based on the Wesenheit-index assuming the slope observed in the LMC, and no metallicity correction. The DM range from 18.45 ± 0.18 to 18.86 ± 0.12. Several important conclusions may be drawn:

(1) For every combination, the PL-relation in K gives the shortest distance, and the difference between the distance based on V and K can be as large as 0.24 mag (solutions 4, 5 in Table 8).

This systematic effect is worrying and merits investigation. It could hint to errors in the reddening, or dereddening procedure. It is illustrative to note that the (minimum, maximum, mean) extinction for the whole sample is $(-0.21, 3.4, 1.3)$ in $A_{\rm V}$, $(-0.08, 2.1, 0.75)$ in $A_{\rm I}$, and $(-0.05, 0.26, 0.10)$ in $A_{\rm K}$. This implies that any uncertainty in reddening is less in K. In Sect. 5.1 we have estimated these uncertainties (about 0.04 in V, 0.03 in I and 0.01 mag in K) and added them as a random errors. Possibly these are errors of a systematic nature instead. It is interesting to note that application of the procedures outlined in Sect. 3.2 results in negative reddening in some cases.

One can raise the question how much bluer the period-colour-relations need to be to give positive reddening for all stars. It turns out that Eq. (4) needs to be bluer by 0.065 mag, Eq. (8) by 0.055 mag, and Eq. (11) by 0.075 mag. For the default slopes and using all stars, the zero points in V, I, K would change to, respectively, -1.620 (from -1.411), -1.970 (from -1.892), and -2.660 (from -2.607).

On the other hand, the DM based on the Wesenheit-index, which avoids the use of a PC-relation to estimate the individual reddenings, is in perfect agreement with the DM based both on the PL-relations in V and I. This suggests that the reddening is not the main reason for the systematically shorter DM in the K-band.

As pointed out in Sect. 4.3 there may be a bias in the K-band zero point due to the smaller number of Cepheids with accurate intensity-mean magnitudes. The correction for this bias was estimated by comparing, for the same sample of stars with K-band data, the zero point of the PL-relations in V and I to those for the full samples in V and I, and this correction is about 0.1 mag, in the sense that it makes the DM based on K shorter than they would be without this correction. This uncertainty can only be eliminated if more intensity-mean NIR magnitudes come available.

(2) The uncertainty in the type of metallicity correction introduces a range in DM of up to 0.20 mag in V, I, and 0.12 mag in K.

(3) The uncertainty in the slope of the Galactic PL-relations introduces a range in DM of about 0.16 mag in V, I, and about 0.05 mag in K.

Taking the case with the observed slopes of LMC Cepheids with no metallicity correction as default, one may summarise the results as follows. Based on the PL-relation in V and I, and the Wesenheit-index, the true DM to the LMC is 18.60 ± 0.11 (± 0.08 slope) ($^{+0.08}_{-0.15}$ metallicity). Based on the PL-relation in K it is 18.52 ± 0.18 (± 0.03 slope) (± 0.06 metallicity) ($^{+0.10}_{-0}$ sample bias). The terms between parenthesis indicate the possible systematic uncertainties due to the slope of the Galactic PL-relations, the metallicity corrections, and in the K-band, due to the limited number of stars. Recent work by Sandage et al. (1999) indicate that the effect of metallicity towards shorter distances may be smaller in V and I than indicated here. A more accurate determination is not possible without more definite information on the slope of the Galactic PL-relations and the metallicity correction.

Our prefered distance modulus is the one based on the PL-relation in V, I and the Wesenheit index, and puts the LMC 0.10 mag in DM closer than the value of 18.70 derived by FC. The difference is due to four effects that all work in the same direction, namely, (1) FC apply a metallicty correction of +0.042 mag, (2) the difference in the zero point in the Galactic PL-

relation in V between FC and this study is +0.03 mag (+0.01 mag is due to Malmquist bias which FC did not take into account, while +0.02 mag is due to the different sample and slightly different photometry in some cases), (3) the difference in the DM based on V compared to the mean of the DM based on V, I and the Wesenheit-index is +0.02 mag, and (4) the difference between FC and this study in the adopted zero point of the PL-relation in V of the LMC Cepheids is +0.01 mag.

We finally note that the influence of the choice of slope and the metallicity correction are (predicted to be) smallest in the K-band as well as the uncertainty in the extinction correction. If the 20-30 closest Cepheids without published NIR photometry could have their NIR intensity-mean magnitudes determined, then the uncertainty due to the small number of stars could be eliminated and the zero point in K could be determined with an error that is a factor of two smaller than is possible at present.

Acknowledgements. We thank Pascal Fouqué, Michael Feast and Patricia Whitelock for providing tabular material in Gieren et al. (1998), respectively Feast & Whitelock (1997) in electronic format. We thank Giuseppe Bono and Santi Cassisi in calculating and communicating additional $PL(C)$-relations to us. Frederic Pont and Frederic Arenou are thanked for lively and interesting discussions. This research has made use of the SIMBAD database, operated at CDS, Strasbourg, France.

Appendix

In this appendix we list the sample of 236 Cepheids in the HIPPARCOS catalog considered in this study. Listed in Table A1 are the HIP number and variable star name, the parallax and error in the parallax from the HIPPARCOS catalog except for RY Sco and Y Lac (Falin & Mignard 1999), the intensity-mean V and $B-V$ adopted, the $\log$ of the fundamental period, and the assumed pulsation mode. The $V-I$ colours and JHK photometry can be found in G99, as described in Sect. 2.

References

Alcock C., Allsman R.A., Axelrod T.S., et al., 1995, AJ 109, 1653
Alcock C., Allsman R.A., Alves D.R., et al., 1999, AJ 117, 920
Alibert Y., Baraffe I., Hauschildt P., Allard F., 1999, A&A 344, 551
Andrievsky S.M., Kovtyukh V.V., Bersier D., et al., 1998, A&A 329, 599
Antonello E., Poretti E., Reduzzi L., 1990, A&A 236, 138
Arenou F., Grenon M., Gomez A., 1992, A&A 258, 104
Arenou F., Lindegren L., Froeschlé, M., et al., 1995, A&A 304, 52
Bauer F., Afonso C., Albert J.N., et al., 1999, A&A 348, 175
Berdnikov L.N., Turner D.G., 1995, Pis'ma Astr. J. 21, 803
Bono G., Caputo F., Castellani V., Marconi M., 1999, ApJ 512, 711
Brown A.G.A., Arenou F., van Leeuwen F., Lindegren L., Luri X., 1997, In: Patrick B. (ed.) Hipparcos, Venice 1997, ESA-SP 402, p. 63
Caldwell J.A.R., Coulson I.M., 1986, MNRAS 218, 223
Caldwell J.A.R., Coulson I.M., 1987, AJ 93, 1090
Caldwell J.A.R., Laney C.D., 1991, In: Haynes R., Milne D. (eds.) IAU symposium 148: The Magellanic Clouds. Kluwer, p. 249
ESA, 1989, The Hipparcos Mission. Volume II: The Input Catalogue. ESA SP-1111, Vol. II
ESA, 1997, The Hipparcos and Tycho Catalogues. ESA SP-1200
Falin J.L., Mignard F., 1999, A&AS 135, 231
Feast M.W., 1999, PASP 111, 775
Feast M.W., Catchpole R.M., 1997, MNRAS 286, L1 (FC)
Feast M.W., Whitelock P.A., 1997, MNRAS 291, 683
Fernie J.D., Beattie B., Evans N.R., Seager S., 1995, IBVS 4148 (F95)
Gibson B.K., Stetson P.B., Freedman W.L., et al., 1999, astro-ph/9908149
Gieren W.P., Fouqué P., Gómez M., 1998, ApJ 496, 17
Groenewegen M.A.T, 1999, A&AS 139, 245 (G99)
Kennicutt R.C., Stetson P.B., Saha A., et al., 1998, ApJ 498, 181
Kochanek C.S., 1997, ApJ 491, 13
Koen C., 1992, MNRAS 256, 65
Koen C., Laney D., 1998, MNRAS 301, 582
Laney C.D., 1999, In: Whitelock P., Cannon R. (eds.) IAU symposium 192: The Stellar Content of the Local Group. p. 459
Laney C.D., 2000, In: IAU Coll. 176: The impact of large-scale surveys on variable star research.
Laney C.D., Stobie R.S., 1993, MNRAS 263, 921
Laney C.D., Stobie R.S., 1994, MNRAS 266, 441
Lanoix P., Paturel G., Garnier R., 1999, MNRAS 308, 969 (L99)
Luri X., Torra J., Figueras F., et al., 1999, In: Egret D., Heck A. (eds.) Harmonizing Distance scales in a post-Hipparcos Era. ASP Conf. Ser. 167, p. 33
Lutz T.E., Kelker D.H., 1973, PASP 85, 573
Madore B., Freedman W.L., 1991, PASP 103, 933
Mantegazza L., Poretti E., 1992, A&A 261, 137
Moffett T.J., Barnes T.G., 1984, ApJS 55, 389
Oudmaijer R.D., Groenewegen M.A.T., Schrijver H., 1998, MNRAS 294, L41
Oudmaijer R.D., Groenewegen M.A.T., Schrijver H., 1999, A&A 341, L55
Pont F., 1999, In: Egret D., Heck A. (eds.) Harmonizing Distance scales in a post-Hipparcos Era. ASP Conf. Ser. 167, p. 113
Robichon N., Arenou F., Mermilliod J.-C., Turon C., 1999, A&A 345, 471
Sachkov M.E., 1997, IBVS 4522
Saio H., Gautschy A., 1998, ApJ 498, 360
Sandage A., 1994, ApJ 430, 1
Sandage A., Bell R.A., Tripicco M.J., 1999, ApJ 522, 250
Sasselov D.D., Beauliau J.P., Renault C., et al., 1997, A&A 324, 471
Sekiguchi M., Fukugita M., 1998, Observatory 118, 73
Smith H. Jr., 1987a, A&A 171, 336
Smith H. Jr., 1987b, A&A 171, 342
Smith H. Jr., 1987c, A&A 181, 391
Stobie R.S., Ishida K., Peacock J.A., 1989, MNRAS 238, 709
Storm J., Carney B.W., Fry A.M., 1999, In: Egret D., Heck A. (eds.) Harmonizing Distance scales in a post-Hipparcos Era. ASP Conf. Ser. 167, p. 320
Storm J., 2000, In: IAU Coll. 176: The impact of large-scale surveys on variable star research
Tanvir N.R., 1999, In: Egret D., Heck A. (eds.) Harmonizing Distance scales in a post-Hipparcos Era. ASP Conf. Ser. 167, p. 84
Turon Lacarrieu C., Crézé M., 1977, A&A 56, 273
Van Hoolst T., Waelkens C., 1995, A&A 295, 361
Van Leeuwen F., 1997, Space Sci. Rev. 81, 208

Table A1. The sample of HIPPARCOS Cepheids

HIP	Name	π (mas)	σ_π (mas)	V	$(B-V)$	$\log P_0$	mode
1162	FM Cas	0.10	1.27	9.127	0.989	0.764	0
1213	SY Cas	2.73	1.49	9.868	0.992	0.610	0
2347	DL Cas	2.32	1.09	8.969	1.154	0.903	0
3886	XY Cas	-0.02	1.58	9.935	1.147	0.653	0
5138	VW Cas	-2.12	3.61	10.697	1.245	0.778	0
5658	UZ Cas	4.37	3.64	11.338	1.110	0.629	0
5846	BP Cas	-0.60	2.04	10.920	1.550	0.798	0
7192	V636 Cas	1.72	0.81	7.199	1.365	0.923	0
7548	RW Cas	0.69	1.68	9.217	1.196	1.170	0
8312	BY Cas	-0.85	3.25	10.366	1.309	0.662	1
8614	VV Cas	-4.78	4.18	10.724	1.143	0.793	0
9928	VX Per	1.08	1.48	9.312	1.158	1.037	0
11174	V440 Per	1.62	0.83	6.282	0.873	1.039	1
11420	SZ Cas	2.21	1.60	9.853	1.419	1.135	0
11767	α UMi	7.56	0.48	1.982	0.598	0.754	1
12817	DF Cas	-0.27	3.65	10.848	1.181	0.584	0
13367	SU Cas	2.31	0.58	5.970	0.703	0.440	1
19978	SX Per	-1.59	2.96	11.158	1.155	0.632	0
20202	AS Per	0.56	1.84	9.723	1.302	0.697	0
21517	SZ Tau	3.12	0.82	6.531	0.844	0.651	1
22445	SV Per	-3.32	1.54	9.020	1.029	1.046	0
23210	AN Aur	-1.19	2.34	10.455	1.218	1.012	0
23360	RX Aur	1.32	1.02	7.655	1.009	1.065	0
23768	CK Cam	-0.33	0.95	7.541	0.990	0.518	0
24105	BK Aur	0.47	1.38	9.427	1.062	0.903	0
24281	SY Aur	1.15	1.70	9.074	1.000	1.006	0
24500	YZ Aur	3.70	2.10	10.332	1.375	1.260	0
25642	Y Aur	-0.40	1.47	9.607	0.911	0.586	0
26069	β Dor	3.14	0.59	3.731	0.807	0.993	0
27119	ST Tau	3.15	1.17	8.217	0.847	0.606	0
27183	EU Tau	0.86	1.38	8.093	0.664	0.473	1
28625	RZ Gem	1.90	1.97	10.007	1.025	0.743	0
28945	AA Gem	-2.25	2.42	9.721	1.061	1.053	0
29022	CS Ori	-0.54	3.36	11.381	0.924	0.590	0
29386	GQ Ori	4.77	1.13	8.965	0.976	0.935	0
30219	SV Mon	-1.18	1.14	8.219	1.048	1.183	0
30286	RS Ori	2.02	1.45	8.412	0.945	0.879	0
30827	RT Aur	2.09	0.89	5.446	0.595	0.572	0
31306	DX Gem	-2.58	2.49	10.746	0.936	0.650	1
31404	W Gem	0.86	1.16	6.950	0.889	0.898	0
31624	CV Mon	3.76	2.77	10.299	1.297	0.731	0
31905	BE Mon	-0.28	2.12	10.578	1.134	0.432	0
32180	AD Gem	-0.18	1.60	9.857	0.694	0.578	0
32516	V508 Mon	-2.42	2.28	10.518	0.898	0.616	0
32854	TX Mon	0.00	2.47	10.960	1.096	0.940	0
33014	EK Mon	-0.77	2.69	11.048	1.195	0.598	0
33520	TZ Mon	1.61	2.12	10.761	1.116	0.871	0
33791	AC Mon	0.90	1.94	10.067	1.165	0.904	0
33874	V526 Mon	3.43	1.12	8.597	0.593	0.579	1
34088	ζ Gem	2.79	0.81	3.918	0.798	1.007	0
34421	V465 Mon	2.28	1.88	10.379	0.762	0.586	1
34527	TV CMa	0.90	1.97	10.582	1.175	0.669	0
34895	RW CMa	3.12	2.16	11.096	1.225	0.758	0
35212	RY CMa	0.96	1.09	8.110	0.847	0.670	0
35665	RZ CMa	-1.95	1.51	9.697	1.004	0.629	0
35708	TW CMa	1.26	1.51	9.561	0.970	0.845	0
36125	VZ CMa	1.58	1.65	9.383	0.957	0.495	0
36617	VW Pup	-5.65	2.83	11.365	1.065	0.632	0
36685	X Pup	-0.05	1.10	8.460	1.127	1.414	0

Table A1. (continued)

HIP	Name	π (mas)	σ_π (mas)	V	$(B-V)$	$\log P_0$	mode
37174	MY Pup	0.65	0.52	5.677	0.631	0.913	1
37207	VZ Pup	1.49	1.47	9.621	1.162	1.365	0
37506	EK Pup	3.54	2.34	10.664	0.816	0.571	1
37511	WW Pup	2.07	1.91	10.554	0.874	0.742	0
37515	WX Pup	-1.05	1.08	9.063	0.968	0.951	0
38063	AD Pup	-4.05	1.74	9.863	1.049	1.133	0
38907	AP Pup	1.07	0.64	7.371	0.838	0.706	0
38944	WY Pup	0.11	2.09	10.569	0.791	0.720	0
38965	AQ Pup	8.85	4.03	8.669	1.337	1.479	0
39010	LS Pup	3.90	2.71	10.442	1.231	1.151	0
39144	WZ Pup	-0.55	1.77	10.326	0.789	0.701	0
39666	BN Pup	4.88	1.72	9.882	1.186	1.136	0
39840	LX Pup	3.08	2.59	10.630	1.032	1.142	0
40078	HL Pup	-10.42	4.30	10.740	0.862	0.542	0
40155	AH Vel	2.23	0.55	5.695	0.579	0.782	1
40178	AT Pup	1.20	0.74	7.957	0.783	0.824	0
40233	RS Pup	0.49	0.68	7.028	1.434	1.617	0
41588	V Car	0.34	0.58	7.362	0.872	0.826	0
42257	RZ Vel	1.35	0.63	7.079	1.120	1.310	0
42321	T Vel	0.48	0.72	8.024	0.922	0.666	0
42831	SW Vel	1.30	0.90	8.120	1.162	1.370	0
42926	SX Vel	1.54	0.79	8.251	0.888	0.980	0
42929	ST Vel	-1.62	0.99	9.704	1.195	0.768	0
44847	BG Vel	1.33	0.65	7.635	1.175	0.999	1
45570	DK Vel	-1.70	3.78	10.614	0.774	0.546	1
45949	W Car	1.16	0.63	7.589	0.788	0.641	0
46746	DR Vel	-0.45	1.07	9.520	1.518	1.049	0
47177	AE Vel	-0.64	1.33	10.262	1.243	0.853	0
47854	l Car	2.16	0.47	3.724	1.299	1.551	0
48122	FN Vel	0.77	1.63	10.430	0.912	0.726	0
48663	GX Car	1.43	1.12	9.364	1.043	0.857	0
50244	CN Car	5.11	1.53	10.700	1.089	0.693	0
50655	RY Vel	-1.15	0.83	8.397	1.352	1.449	0
50722	AQ Car	1.02	0.81	8.851	0.928	0.990	0
51142	UW Car	-0.64	1.12	9.426	0.971	0.728	0
51262	YZ Car	1.79	1.03	8.714	1.124	1.259	0
51338	UX Car	0.00	0.87	8.308	0.627	0.566	0
51894	XX Vel	1.14	1.50	10.654	1.162	0.844	0
51909	UZ Car	-0.70	1.00	9.323	0.875	0.716	0
52157	HW Car	-0.71	1.06	9.163	1.055	0.964	0
52380	EY Car	3.46	1.62	10.318	0.854	0.459	0
52570	SV Vel	-1.27	0.97	8.524	1.054	1.149	0
52661	SX Car	2.48	1.06	9.089	0.887	0.687	0
53083	WW Car	4.23	1.39	9.743	0.890	0.670	0
53397	WZ Car	-0.41	1.14	9.247	1.142	1.362	0
53536	XX Car	-0.63	0.95	9.322	1.054	1.196	0
53589	U Car	-0.04	0.62	6.288	1.183	1.589	0
53593	CY Car	-0.30	1.40	9.782	0.953	0.630	0
53867	FN Car	-1.91	2.48	11.542	1.101	0.661	0
53945	XY Car	-0.62	0.95	9.295	1.214	1.095	0
54101	XZ Car	-0.30	0.96	8.601	1.266	1.221	0
54543	ER Car	1.36	0.69	6.824	0.867	0.887	0
54621	GH Car	0.43	1.03	9.177	0.932	0.915	1
54659	V898 Cen	-0.32	0.73	8.000	0.574	0.547	0
54715	IT Car	1.00	0.82	8.097	0.990	0.877	0
54862	GI Car	-0.41	1.10	8.323	0.739	0.802	1
54891	FR Car	0.35	1.29	9.661	1.121	1.030	0
55726	AY Cen	-0.24	1.04	8.830	1.009	0.725	0
55736	AZ Cen	-0.20	1.04	8.636	0.653	0.660	1

Table A1. (continued)

HIP	Name	π (mas)	σ_π (mas)	V	$(B-V)$	$\log P_0$	mode
56176	V419 Cen	1.72	0.93	8.186	0.758	0.898	1
57130	KK Cen	-1.84	2.89	11.480	1.282	1.086	0
57260	RT Mus	1.13	0.99	9.022	0.834	0.489	0
57884	BB Cen	2.85	1.27	9.781	1.150	1.066	0
57978	UU Mus	3.03	1.43	10.073	0.953	0.757	1
59575	AD Cru	1.87	2.32	11.051	1.279	0.806	0
60259	T Cru	0.86	0.62	6.566	0.922	0.828	0
60455	R Cru	1.97	0.82	6.766	0.772	0.765	0
61136	BG Cru	1.94	0.57	5.487	0.606	0.678	1
61981	R Mus	1.69	0.59	6.298	0.757	0.876	0
62986	S Cru	1.34	0.71	6.600	0.761	0.671	0
63693	V496 Cen	1.61	1.53	9.966	1.172	0.646	0
64969	V378 Cen	0.96	1.02	8.460	1.035	0.969	1
65970	V659 Cen	0.75	1.28	6.598	0.758	0.750	0
66189	VW Cen	-2.02	3.63	10.245	1.345	1.177	0
66383	KN Cen	-1.38	2.82	9.870	1.582	1.532	0
66696	XX Cen	2.04	0.94	7.818	0.983	1.039	0
67566	V381 Cen	1.13	0.91	7.653	0.792	0.706	0
70203	V339 Cen	0.33	1.16	8.753	1.191	0.976	0
71116	V Cen	0.05	0.82	6.836	0.875	0.740	0
71492	V737 Cen	3.71	0.84	6.719	0.999	0.849	0
72264	BP Cir	0.13	0.88	7.560	0.702	0.531	1
72583	AV Cir	3.40	1.09	7.439	0.910	0.640	1
74448	IQ Nor	-0.24	3.08	9.566	1.314	0.916	0
75018	R TrA	0.43	0.71	6.660	0.722	0.530	0
75430	GH Lup	2.65	0.86	7.635	1.210	0.967	0
76918	U Nor	2.52	1.28	9.238	1.576	1.102	0
78476	S TrA	1.59	0.72	6.397	0.752	0.801	0
78797	RS Nor	-0.23	1.81	10.027	1.287	0.792	0
79625	GU Nor	4.45	2.06	10.411	1.273	0.538	0
79932	S Nor	1.19	0.75	6.426	0.945	0.989	0
82023	V340 Ara	0.06	2.12	10.164	1.539	1.318	0
82498	KQ Sco	0.07	2.31	9.807	1.934	1.458	0
83059	RV Sco	2.54	1.13	7.040	0.955	0.783	0
83674	BF Oph	1.17	1.01	7.337	0.868	0.609	0
85035	V636 Sco	-0.45	0.89	6.654	0.936	0.832	0
85701	V482 Sco	-0.45	1.16	7.965	0.975	0.656	0
86269	V950 Sco	2.46	1.04	7.302	0.775	0.683	1
87072	X Sgr	3.03	0.94	4.549	0.739	0.846	0
87173	V500 Sco	2.21	1.30	8.729	1.276	0.969	0
87345	RY Sco	0.96	2.70	8.004	1.426	1.308	0
87495	Y Oph	1.14	0.80	6.169	1.377	1.234	0
89013	CR Ser	-3.04	2.08	10.842	1.644	0.724	0
89276	AP Sgr	-0.95	0.92	6.955	0.807	0.704	0
89596	WZ Sgr	-0.75	1.76	8.030	1.392	1.339	0
89968	Y Sgr	2.52	0.93	5.744	0.856	0.761	0
90110	AY Sgr	-0.99	2.28	10.549	1.457	0.817	0
90241	XX Sgr	2.64	1.22	8.852	1.107	0.808	0
90791	X Sct	0.97	1.46	10.006	1.140	0.623	0
90836	U Sgr	0.27	0.92	6.695	1.087	0.829	0
91239	EV Sct	0.91	1.92	10.137	1.160	0.643	1
91366	Y Sct	0.00	1.69	9.628	1.539	1.015	0
91613	CK Sct	3.62	2.12	10.590	1.566	0.870	0
91697	RU Sct	0.89	1.61	9.466	1.645	1.294	0
91706	TY Sct	4.02	2.27	10.831	1.657	1.043	0
91738	CM Sct	-3.72	2.35	11.106	1.371	0.593	0
91785	Z Sct	1.14	1.66	9.600	1.330	1.111	0
91867	SS Sct	-1.07	1.17	8.211	0.944	0.565	0
92370	YZ Sgr	0.87	1.03	7.358	1.032	0.980	0

Table A1. (continued)

HIP	Name	π (mas)	σ_π (mas)	V	$(B-V)$	$\log P_0$	mode
92491	BB Sgr	0.61	0.99	6.947	0.987	0.822	0
93063	V493 Aql	-2.77	2.43	11.083	1.280	0.475	0
93124	FF Aql	1.32	0.72	5.372	0.756	0.806	1
93399	V336 Aql	0.75	1.47	9.848	1.312	0.864	0
93681	SZ Aql	0.20	1.10	8.599	1.389	1.234	0
93990	TT Aql	0.41	0.96	7.141	1.292	1.138	0
94004	V496 Aql	-3.81	1.05	7.751	1.146	0.833	0
94094	FM Aql	2.45	1.11	8.270	1.277	0.786	0
94402	FN Aql	1.53	1.18	8.382	1.214	1.138	1
94685	V473 Lyr	1.94	0.62	6.182	0.632	0.433	2
95118	V600 Aql	1.42	1.80	10.037	1.462	0.860	0
96458	U Vul	0.59	0.77	7.128	1.275	0.903	0
96596	V924 Cyg	0.83	1.64	10.710	0.847	0.746	0
97309	BR Vul	-2.80	1.70	10.687	1.474	0.716	0
97439	V1154 Cyg	0.88	0.88	9.190	0.925	0.692	0
97717	SV Vul	0.79	0.74	7.220	1.442	1.653	0
97794	V1162 Aql	0.15	1.15	7.798	0.879	0.888	1
97804	η Aql	2.78	0.91	3.897	0.789	0.856	0
98085	S Sge	0.76	0.73	5.622	0.805	0.923	0
98212	X Vul	-0.33	1.10	8.849	1.389	0.801	0
98376	GH Cyg	1.93	1.67	9.924	1.266	0.893	0
98852	CD Cyg	0.46	1.00	8.947	1.266	1.232	0
99276	V402 Cyg	1.19	1.18	9.873	1.008	0.640	0
99567	MW Cyg	-1.63	1.30	9.489	1.316	0.775	0
99887	V495 Cyg	-0.95	1.32	10.621	1.623	0.827	0
101393	SZ Cyg	0.86	1.09	9.432	1.477	1.179	0
102276	X Cyg	1.47	0.72	6.391	1.130	1.214	0
102949	T Vul	1.95	0.60	5.754	0.635	0.647	0
103241	V520 Cyg	1.51	1.73	10.851	1.349	0.607	0
103433	VX Cyg	0.88	1.43	10.069	1.704	1.304	0
103656	TX Cyg	0.50	1.09	9.511	1.784	1.168	0
104002	VY Cyg	-0.02	1.44	9.593	1.215	0.895	0
104185	DT Cyg	1.72	0.62	5.774	0.538	0.549	1
104564	V459 Cyg	0.51	1.50	10.601	1.439	0.860	0
104877	V386 Cyg	2.22	1.17	9.635	1.491	0.721	0
105369	V532 Cyg	0.84	0.94	9.086	1.036	0.516	0
106754	V538 Cyg	0.10	1.52	10.456	1.283	0.787	0
107899	VZ Cyg	2.84	1.17	8.959	0.876	0.687	0
108426	IR Cep	1.38	0.61	7.784	0.888	0.476	1
108427	CP Cep	1.54	1.52	10.590	1.668	1.252	0
108630	BG Lac	-0.35	1.31	8.883	0.949	0.727	0
109340	Y Lac	0.45	1.70	9.146	0.731	0.636	0
110964	AK Cep	0.22	2.52	11.180	1.341	0.859	0
110968	V411 Lac	0.67	0.70	7.860	0.741	0.464	0
110991	δ Cep	3.32	0.58	3.954	0.657	0.730	0
111972	Z Lac	2.04	0.89	8.415	1.095	1.037	0
112026	RR Lac	0.94	0.95	8.848	0.885	0.807	0
112430	CR Cep	1.67	1.06	9.656	1.396	0.795	0
112626	V Lac	0.34	0.85	8.936	0.873	0.697	0
112675	X Lac	0.57	0.79	8.407	0.901	0.893	1
114160	SW Cas	1.07	1.37	9.705	1.081	0.736	0
115390	CH Cas	0.21	1.68	10.973	1.650	1.179	0
115925	CY Cas	2.76	3.21	11.641	1.738	1.158	0
116556	RS Cas	2.43	1.24	9.932	1.490	0.799	0
116684	DW Cas	1.19	1.95	11.112	1.475	0.699	0
117154	CD Cas	1.91	1.58	10.738	1.449	0.892	0
117690	RY Cas	0.02	1.38	9.927	1.384	1.084	0
118122	DD Cas	0.57	1.14	9.876	1.188	0.992	0
118174	CF Cas	-3.20	2.16	11.136	1.174	0.688	0